

1 **Variability of the Apparent Respiratory Quotient of a forest Soils and Tree**
 2 **Stems**

3 **Boaz Hilman^{1,2}, Tal Weiner¹, Tom Haran¹, and Alon Angert¹**

4 ¹ The Institute of Earth Sciences, The Hebrew University of Jerusalem, Givat-Ram, Jerusalem
 5 91904, Israel

6 ² Department of Biogeochemical Processes, Max-Planck Institute for Biogeochemistry, Jena,
 7 07745, Germany

8 Corresponding author: Boaz Hilman (bhilman@bgc-jena.mpg.de)

9 **Key Points:**

- 10 • The ratio of CO₂/O₂ fluxes in respiration (ARQ) depends on the substrate stoichiometry
 11 and on additional processes reacting with the gases
- 12 • Bulk-soil ARQ value is governed by stoichiometry in high respiration rates and by
 13 processes like abiotic Fe²⁺ oxidation in low rates
- 14 • ARQ can be used to partition soil respiration sources as shown by distinct bulk-soil and
 15 roots ARQ values that confine total soil value
- 16

17 Abstract

18 The CO₂/O₂ fluxes ratio (ARQ) measured in soils and plants contains valuable information about
19 the respiratory-substrate stoichiometry and biotic and abiotic non-respiratory processes reacting
20 with the gases. For meaningful use in biogeochemical studies it is necessary to resolve the
21 substrate and processes effects. In addition, unique ARQ signatures can be used to weight
22 contributions to soil respiration. We investigated these uses by measurements in soil pore space
23 air (ARQ_{sa}), and in headspace air from incubations of bulk-soil (ARQ_{bs}) and tree stem-tissues
24 (ARQ_{ts} for fresh tissues; ARQ_{ts24} after 24-h storage) in 10 measurement campaigns over 15
25 months in a Mediterranean oak forest. Mean (range) values were: ARQ_{sa} = 0.76 (0.60-0.92),
26 ARQ_{bs} = 0.75 (0.53-0.90), ARQ_{ts} = 0.39 (0.19-0.70), and ARQ_{ts24} = 0.68 (0.42-1.08). Both
27 ARQ_{ts} and ARQ_{ts24} were below 1.0, the value expected for carbohydrate respiration in plants.
28 Involvement of non-respiratory processes like non-phototrophic CO₂ re-fixation and wound-
29 response O₂ uptake (for ARQ_{ts}) can explain the results. The mean ARQ_{bs} (0.75) probably
30 represents the stoichiometry of the respiratory substrate, which is lower than expected using bulk
31 soil organic matter (SOM) stoichiometry (~0.95), suggesting a labile, less oxidized, SOM pool
32 contributes more to respiration fluxes. Abiotic O₂ uptake by Fe²⁺ was demonstrated to reduce
33 ARQ_{bs} to 0.37, at the most, but estimated to have small effect under typical respiration rates.
34 ARQ_{sa} was usually higher than ARQ_{bs} and lower than root ARQ (which, when measured, ranged
35 from 0.73-0.96), demonstrating the potential of ARQ to partition the autotrophic and
36 heterotrophic sources of soil respiration.

37

38 Plain Language Summary

39 Carbon dioxide is produced by the processes of both metabolic respiration by plants and
40 microbial respiration and decomposition in soils. These are among the most important processes
41 in terrestrial ecosystems, both oxidizing organic compounds using O₂ and emitting the resulting
42 CO₂ to the atmosphere. However, our understanding of these processes, which are often
43 collectively referred to as “respiration” is still incomplete. Here we investigated the use of the
44 measured ratio CO₂ released to O₂ consumed, termed the apparent respiration quotient (ARQ), to
45 investigate respiration in soils and tree stems. ARQ measurements are rarely made, but can
46 provide valuable information about the chemistry of the respiratory substrates, and about
47 additional processes that involve CO₂ and O₂ cycling in terrestrial ecosystems. The expected
48 substrates (carbohydrates) in tree stems and soils yield ARQ ≈ 1; however, we measured
49 considerably lower values. The low ARQ values in the soil can be explained if microbes
50 decompose compounds with low amounts of oxygen, which is surprising. No substrates can
51 produce ARQ values as low as those we measured in stem core incubations, indicating another
52 processes at work.

53

54

55

56

57

58 1 Introduction

59 New measurement methods can improve the understating and prediction of ecosystem processes.
60 An emerging tool in biogeochemical studies is the coupled measurement of CO₂ and O₂ fluxes.
61 In respiration the ratio CO₂ production/O₂ consumption is termed the ‘respiratory quotient’ (RQ).
62 The inverse term ‘oxidative ratio’ (OR, 1/RQ) is also used, especially when describing
63 ecosystem processes that include photosynthesis with O₂ production (where the fluxes direction
64 is opposite to respiration). Both ratios depend primarily on the stoichiometry, of the respiratory
65 substrate or the net synthesized biomass. The stoichiometry of organic molecule determines the
66 mean oxidation state (C_{ox}) of the C atoms in the molecule [LaRowe and Van Cappellen, 2011;
67 Masiello *et al.*, 2008]. The more oxidized (higher C_{ox}) the molecule, the fewer moles of O₂ are
68 consumed per mole of CO₂ released during complete oxidation and the RQ is higher (Table 1).
69 For this reason RQ is often used to infer which respiratory substrate is being used by plants and
70 animals. However, in soils and isolated plant organs additional biotic and abiotic non-respiratory
71 processes can influence CO₂ and/or O₂ and lead to a ratio of CO₂/O₂ that differs from the change
72 the substrate’s RQ value. For this reason, we refer to the ratio CO₂ efflux/O₂ uptake measured in
73 tree stems and soils as the ‘apparent RQ’ (ARQ) [Angert and Sherer, 2011; Angert *et al.*, 2015].
74 The main processes with the potential to affect ARQ are presented in Figure 1 and detailed in
75 section 1.1. In addition, in a recent study we suggested that ARQ measurements could be used to
76 separate autotrophic and heterotrophic respiration sources in soils due to different ARQ
77 signatures [Hicks Pries *et al.*, 2019]. Thus, ARQ has the potential to become a useful tracer,
78 similar to δ¹³C in the ability to identify respiratory substrates, processes, and to separate
79 respiration sources [M E Gallagher *et al.*, 2017].

80 For meaningful use of ARQ as a biogeochemical tracer, it is crucial to identify and
81 separate the signals related to substrate stoichiometry and to non-respiratory processes. In
82 addition, the sources of ARQ variability in soils and tree stems are still unclear. Addressing these
83 questions has become more feasible with the development of user friendly O₂ sensors based on
84 fuel-cell and optical quenching technologies. In the current study we explore ARQ variability
85 and its sources in soils and tree stems of a Mediterranean oak forest, and discuss next research
86 steps.

87

88

89

90

91

92

93

94

95

96

97

98 Table 1 – Selected Compounds and their Type, Formula, Mean Oxidation State of the C (C_{ox}),
 99 RQ, OR, and the Gibbs Energy.

Compound	Type	Formula	C_{ox}^a	RQ (ARQ) ^b	OR ^c	Gibbs energy (kJ mol C ⁻¹) ^d
Oxalic acid	Organic acid	C ₂ H ₂ O ₄	3	4	0.25	-25.2
Glucose	Carbohydrate	C ₆ H ₁₂ O ₆	0	1	1	60.3
Cellulose	Structural polysaccharide	(C ₆ H ₁₀ O ₅) _n	0	1	1	60.3
Aspartic acid	Amino acid	C ₄ H ₇ NO ₄	1	1.33 (NH ₃) 0.80 (HNO ₃)	0.75 (NH ₃) 1.25 (HNO ₃)	31.8
Lignin ^e	Structural polymer	C ₁₀₀ H ₁₂₄ O ₄₃	-0.38	0.91	1.10	71.13
Oleic acid	Fatty acid (lipid)	C ₁₈ H ₃₄ O ₂	-1.66	0.71	1.42	107.8
Methane	Inorganic gas	CH ₄	-4	0.5	2	174.3

100 ^a The mean oxidation state of C in the molecule, known also as NOSC (the average nominal
 101 oxidation state of carbon) calculated by $C_{ox} = \frac{2d-b+3c-z}{a}$ where the coefficients are according to
 102 the molecule formula C_aH_bN_cO_d^z while z corresponds to the net charge [LaRowe and Van
 103 Cappellen, 2011; Masiello et al., 2008]. This calculation assumes all non C species have fixed
 104 oxidation state during formation or break down. C_{ox} is related to RQ by $RQ = \frac{4}{4-C_{ox}}$. ^b The
 105 respiratory quotient (RQ), the ratio CO₂ efflux / O₂ uptake in full aerobic oxidation of the
 106 compound. We use the term ARQ (apparent RQ) since in soils and tree stems measurements
 107 additional processes can cause deviation from the theoretic RQ. When molecule contains N the
 108 RQ and OR values depend on the N oxidation state in the respective end and source molecules
 109 (e.g. NH₃ (-3) or HNO₃ (+5)). ^c The oxidative ratio (OR = 1/RQ). Often viewed as the ratio O₂
 110 produced/ CO₂ assimilated required for the biosynthesis of the compound. ^d The Gibbs energy
 111 for oxidation half reactions at 25°C and 1 bar calculated using LaRowe and Van Cappellen's
 112 (2011) Eq. 14: $G_{COx}^0 = 60.3 - 28.5 * C_{ox}$. ^e Lignin formula is according to Baldock et al. 2004.

113 1.1 Observed ARQ in soil respiration components and tree stems

114 The ARQ of soil heterotrophic respiration is usually approximated by root-free bulk-soil
 115 incubations (ARQ_{bs}). According to meta-analysis of C_{ox} in soil organic matter (SOM) [Worrall et
 116 al., 2013] ARQ_{bs} values are expected to range between 0.77 and 1.11 with median of 0.95.
 117 However, values of 0.27-0.94 measured previously from a variety of natural ecosystems and
 118 agricultural lands are mostly below these expected values [Angert et al., 2015; Aon et al., 2001a;
 119 b; Dilly, 2001; 2003; Dilly and Zyakun, 2008; Severinghaus, 1995]. Reasons for measured ARQ
 120 in incubations to differ from the values expected from C_{ox} of bulk soils include (Fig. 1): (1)
 121 processes involving electron transfer that affect either O₂ uptake or CO₂ production without
 122 affecting both gases; (2) interactions involving the greater solubility of CO₂ in water and
 123 inorganic C cycling that do not affect O₂ simultaneously; (3) other processes that affect CO₂

124 more than O₂ or vice versa such enzymatic uptake of CO₂ by ‘dark fixation’ that affect CO₂ more
125 than O₂.

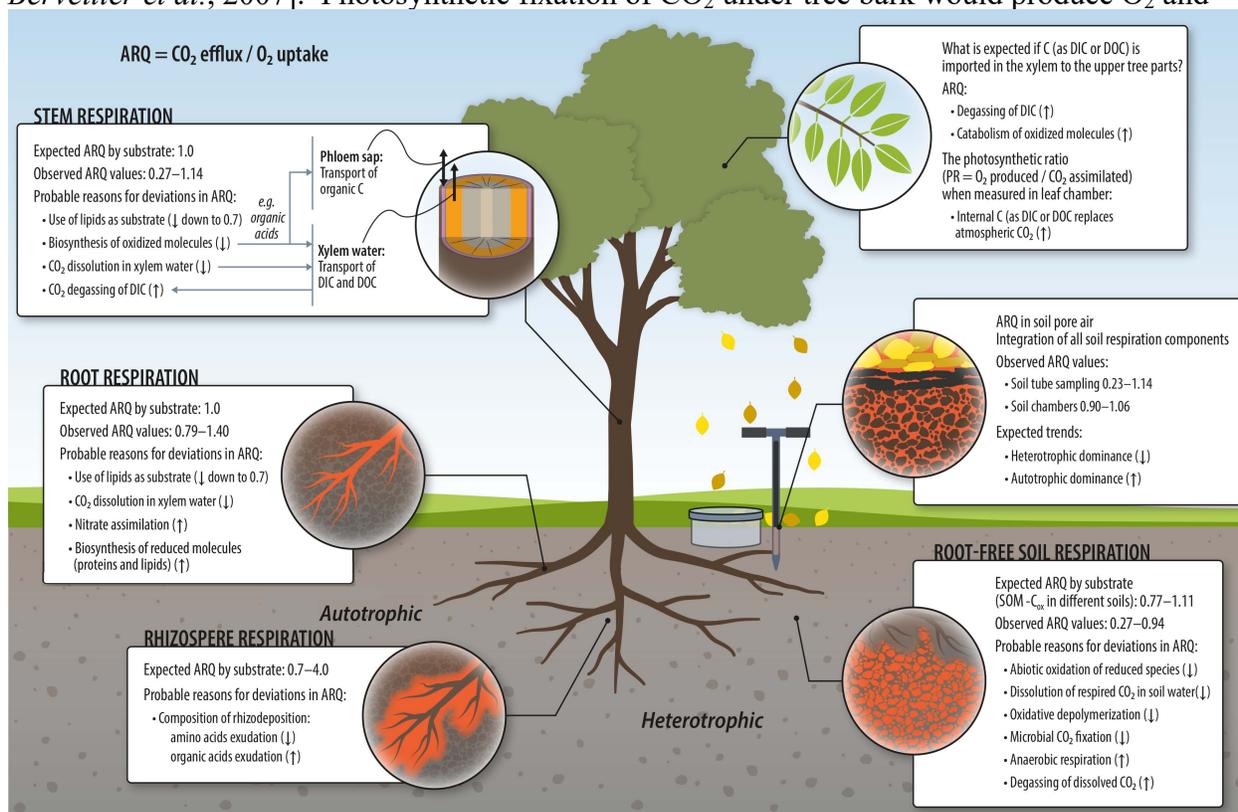
126 Enhanced O₂ uptake derived from abiotic oxidation of reduced species like Fe²⁺ and Mn²⁺
127 increases the denominator of the ARQ ratio and thus decreases its value. The opposite effect on
128 ARQ is expected during anoxic conditions when oxidized Fe³⁺ and Mn³⁺ for example are used as
129 an alternative electron acceptors. In that case, CO₂ is emitted without any O₂ uptake and the
130 numerator of the ARQ ratio increases. Anoxic conditions may exist within soil aggregates even
131 in aerated soils [Druschel *et al.*, 2008; Hall and Silver, 2013; Sexstone *et al.*, 1985], but become
132 more important after soil wetting as diffusion in water is slower by orders of magnitude than
133 diffusion in air, and when respiration rates are high and O₂ replenishment in microsites cannot
134 meet respiratory needs.

135 Carbon dioxide reacts with water to form weak acids (HCO₃⁻ and CO₃²⁻) and is ~30 times
136 more soluble than O₂. Storage of respired CO₂ as dissolved inorganic carbon (DIC) in soil water
137 therefore can also lower the measured ARQ_{bs}, especially in soils that may contain calcium
138 carbonate. At higher soil pH the concentrations of HCO₃⁻ and CO₃²⁻ increase, and therefore also
139 the capacity of the soil water to hold DIC. However, if the water containing the DIC does not
140 leach, the CO₂ is expected to degas back to the soil pore space when the soil is dried. In
141 calcareous soils mainly in arid and semi-arid regions large ARQ_{sa} deviations are expected due to
142 precipitation and dissolution of carbonates [Angert *et al.*, 2015; Benavente *et al.*, 2010; Cuezva *et al.*
143 *et al.*, 2011; Emmerich, 2003; T M Gallagher and Breecker, 2020; Ma *et al.*, 2013].

144 Other processes involving CO₂ and O₂ include root uptake, SOM oxidation processes,
145 and dark fixation. DIC (or CO₂) uptake by roots is probably not substantial due to anatomical
146 features [Ubierna *et al.*, 2009]. ‘Oxidative depolymerization’ is the addition of oxygen to
147 macromolecules that forms smaller and soluble molecules, which are more readily digested by
148 microbes [Kleber *et al.*, 2015]. If the oxygen-rich molecules are not respired and rather bind to
149 mineral surfaces, there is a net O₂ uptake and ARQ is lowered. Dark fixation of CO₂ by the
150 microbial community is another process that can lower ARQ_{bs} [Akinyede *et al.*, 2020; Miltner *et al.*,
151 *et al.*, 2005].

152 In plants, the primary respiration substrates are carbohydrates with ARQ = 1.0 [Hoch *et al.*
153 *et al.*, 2003; Plaxton and Podestá, 2007]. This value is expected for roots, but measurements of
154 instantaneous ARQ from roots (ARQ_{root}) often deviate from 1.0, ranging from 0.79 -1.4
155 [Hawkins *et al.*, 1999; Rachmilevitch *et al.*, 2006; Shane *et al.*, 2004] (Fig. 1). These studies
156 measured ARQ from roots (from intact plants or excised) submerged in nutrient solution.
157 ARQ_{root} values greater than 1.0 were explained by nitrate assimilation that consumes electrons
158 otherwise delivered to O₂ [Bloom *et al.*, 1989; Lambers *et al.*, 2008; Rachmilevitch *et al.*, 2006],
159 or by protein and lipid synthesis in the roots themselves or in the associated mycorrhiza, since
160 the conversion of carbohydrates to more reduced compounds result in ARQ >1.0 [De Vries *et al.*,
161 1974; Hawkins *et al.*, 1999; Shane *et al.*, 2004]. Another process suggested to occur in roots is
162 dissolution of a fraction of the root-respired CO₂ in the xylem water and its transport to above
163 ground tissues in the transpiration stream [Aubrey and Teskey, 2009; Grossiord *et al.*, 2012].
164 This CO₂ removal is expected to reduce ARQ_{root} during the daytime when transpiration is active.
165 The ARQ associated with respiration in the rhizosphere also depends on the composition of the
166 root exudates, which vary greatly in C_{ox} [Bais *et al.*, 2006]; ARQ will be above 1.0 when
167 exudates are dominated by organic acids and below 1.0 when dominated by amino acids (Table
168 1, Fig. 1).

169 Respiration in tree stems is also based on carbohydrates with expected ARQ (ARQ_{ts}) of
 170 1.0. However, the mean ARQ_{ts} measured from stem chambers in tropical, temperate, and
 171 Mediterranean trees was 0.59 and values of 1 were rarely observed [Angert *et al.*, 2012; Hilman
 172 *et al.*, 2019] (Fig. 1). Dissolution and transport of respired CO₂ via the xylem water stream is
 173 thought to influence the CO₂ efflux measured from tree stems [Teskey *et al.*, 2008]. However,
 174 CO₂ transport was found to have only a minor role in explaining low ARQ_{ts} in the investigated
 175 trees [Hilman *et al.*, 2019]. One indication for little effect of CO₂ transport in the xylem water
 176 was that ARQ_{ts} values measured in stem chambers were similar to those measured during
 177 incubation of stem tissues that were clearly detached from the xylem system and unaffected by
 178 transport. An alternative hypothesis for lower than expected ARQ_{ts} values is non-photosynthetic
 179 CO₂ fixation by the enzyme phosphoenolpyruvate carboxylase (PEPC) [Hilman *et al.*, 2019],
 180 which was found to be highly abundant in young tree stems [Berveiller and Damesin, 2007;
 181 Berveiller *et al.*, 2007]. Photosynthetic fixation of CO₂ under tree bark would produce O₂ and
 182



183 Figure 1 Observed ARQ in different ecosystem components with plausible explanations for
 184 deviations from the expected value. The expected ARQ is according to the putative-substrate
 185 stoichiometry (see Table 1): Carbohydrates for respiration in roots and stems; rhizodeposition
 186 composition for rhizosphere respiration, with values indicative of the end-members amino and
 187 organic acids; and soil organic matter composition for root-free soil respiration according to
 188 Worrall *et al.* [2013]. The observed ARQ values are taken from the literature: Stem respiration
 189 [Angert *et al.*, 2012; Angert and Sherer, 2011; Hilman *et al.*, 2019]; Root respiration [Hawkins *et al.*,
 190 1999; Rachmilevitch *et al.*, 2006; Shane *et al.*, 2004]; Root-free soil respiration [Angert *et al.*,
 191 2015; Aon *et al.*, 2001a; b; Dilly, 2001; 2003; Dilly and Zyakun, 2008; Severinghaus, 1995]; Soil
 192 pore air, tube sampling [Angert *et al.*, 2012; Angert *et al.*, 2015; Hicks Pries *et al.*, 2019;
 193 Sanchez-Canete *et al.*, 2018], soil chambers [Ishidoya *et al.*, 2013; Seibt *et al.*, 2004]. Included

195 also are the expected effects on ARQ and the photosynthetic ratio (O_2 produced/ CO_2
 196 assimilated) if C is imported internally to the canopy.

197 **1.2 ARQ as a tool to separate respiration sources in soil and ecosystem**

198 Total soil respiration integrates heterotrophic respiration in root-free soil and the root-associated
 199 rhizosphere with autotrophic respiration by roots. Measurements of ARQ of total soil respiration
 200 (ARQ_{sa}) have been made in two ways. Most frequently, they have been estimated from the
 201 difference in the ratio of CO_2/O_2 in soil air pore space (sampled by a tube) compared to the
 202 CO_2/O_2 of overlying air, corrected for diffusivity differences [Angert *et al.*, 2015]. Using this
 203 method a wide range of values, between 0.23 and 1.14, were measured in a variety of forest soils
 204 from different biomes [Angert *et al.*, 2012; Angert *et al.*, 2015; Hicks Pries *et al.*, 2019; Sanchez-
 205 Canete *et al.*, 2018]. The second measurement monitored simultaneous changes in CO_2 and O_2 in
 206 the headspace of a chamber covering the soil surface. These measurements tend to have higher
 207 ARQ_{sa} values, ranging between 0.90-1.06 [Ishidoya *et al.*, 2013; Seibt *et al.*, 2004]. The large
 208 observed ARQ_{sa} variability can be attributed to two factors: variability in the relative weight of
 209 each of the soil respiration sources, and variability within each of the sources. For example,
 210 Hicks Pries *et al.* [2019] found strong seasonality in ARQ_{sa} in western US forest conifer stand
 211 with summer vs. winter values of 0.89 and 0.70, respectively. The seasonal variation, observed
 212 also in soil air $\delta^{13}CO_2$, was attributed to changes in respiratory substrates that switched between
 213 root-based respiration of more oxidized compounds during summer and bulk-soil respiration of
 214 more reduced compounds during winter (Table 1, Fig. 1). Similarly, greater contributions of
 215 autotrophic respiration and litter decomposition in shallower horizons that are not well-captured
 216 by soil gas sampling tubes might also explain the high ARQ_{sa} measured from soil chambers.
 217 Overall, different ARQ values for different components of soil (or ecosystem) respiration show
 218 promise for its use to partition respiration sources or identify transport of CO_2 between
 219 components.

220 While measured values of ARQ from soils and stems are often < 1 , total ecosystem CO_2
 221 and O_2 fluxes are nearly balanced ($ARQ \sim 1$). Direct estimates of the oxidative ratio ($OR =$
 222 $1/ARQ$) using gas measurements in and above canopies ranged between 0.94 and 1.10 over diel
 223 and annual cycles [Battle *et al.*, 2019; Ishidoya *et al.*, 2013; Seibt *et al.*, 2004; Stephens *et al.*,
 224 2007]. OR over longer time scales can be estimated by the ecosystem's C_{ox} [Keeling, 1988;
 225 Masiello *et al.*, 2008; Severinghaus, 1995]. According to a meta-analysis of total biomass and
 226 SOM- C_{ox} , OR is mostly between 1.00 – 1.13 in 16 global biomes [Worrall *et al.*, 2013].
 227 Therefore, the low ARQ measured in soils and tree stems must be balanced, at least over longer
 228 time scales, by higher ARQ measured elsewhere.

229 The fact that ARQ_{ts} is almost always lower than the expected value of 1 from substrate
 230 carbohydrates may indicate a process that retains respired CO_2 within the stem [Hilman *et al.*,
 231 2019]. If the CO_2 retention in the stem is due to PEPC re-fixation, biosynthesis of compounds
 232 more oxidized than carbohydrates like organic acids are expected [Lambers *et al.*, 2008]. The
 233 catabolism of organic acids results in $ARQ > 1$ (Table 1) that will balance the observed low
 234 ARQ_{ts} where CO_2 is fixed. The high ARQ may appear in the rhizosphere, if organic acids are
 235 exported via the phloem to the roots and transferred to the soil as root exudates [Hoffland *et al.*,
 236 1992; Shane *et al.*, 2004]. Alternatively, the organic acids might be transported upwards in the
 237 xylem water [Schill *et al.*, 1996] and contribute to respiration in the canopy. For example, the

238 organic acid malate can contribute C to leaf photosynthesis [Hibberd and Quick, 2002], and alter
239 the photosynthetic ratio evaluated by leaf O_2/CO_2 fluxes.

240 Another process proposed for CO_2 retention in the stem is CO_2 dissolution in the xylem
241 water. In this case, CO_2 degassing in higher parts of the tree will result in ARQ values that are
242 locally >1.0 . In addition, dissolved CO_2 may contribute to canopy photosynthesis [Bloemen et
243 al., 2013; Stringer and Kimmerer, 1993] in which case it will also affect the photosynthetic.

244 **2 Materials and Methods**

245 In this study, we focused on the seasonal variation of ARQ in soils and tree stems. Seasonal
246 measurements at ~ 1.5 months intervals of in situ ARQ_{sa} estimated from soil gas tubes and a
247 diffusion model, and ARQ_{bs} and ARQ_{ts} using soil and tree stem incubations were conducted in a
248 Mediterranean oak system. After initially performing bulk-soil incubations (ARQ_{bs}) at room
249 temperature, we realized that the different temperatures in the field may affect measured ARQ_{bs} .
250 We therefore performed an additional experiment to test the temperature effect on ARQ_{bs} and
251 used this to correct the ARQ_{bs} results. The evaluation of the control of physical variables (water
252 availability and temperature) on ARQ seasonal variability was performed using a backward
253 selection technique for multiple regressions. ARQ_{sa} was expected to be higher than ARQ_{bs} due to
254 the contribution of root respiration with higher ARQ than in the bulk soil. A direct test was done
255 by comparison of ARQ_{sa} , ARQ_{bs} , and ARQ_{root} sampled at the same time. Additional experiments
256 were conducted to investigate the potential of Fe^{2+} and Mn^{2+} oxidation to reduce ARQ_{bs} .
257 Following the hypothesis that low ARQ_{ts} is the result of CO_2 re-fixation and production of
258 organic acids, we expected anti-correlation between ARQ_{ts} and ARQ_{sa} if the produced organic
259 acids are secreted finally to the rhizosphere as exudates.

260

261 **2.1 Study site**

262 The study took place in Odem Forest, located 950 m a.s.l, 33°13' N, 35°45' E. The climate is
263 Mesic Mediterranean with a mean annual precipitation of 950 mm and summer and winter mean
264 temperatures of 21.3° C and 7.3°C, respectively. The dominant tree species are the evergreen
265 *Quercus calliprinos* Webb (about 75% of the woody cover area) and the winter-deciduous
266 *Quercus boissieri* Reut. (15%) [Kaplan and Gutman, 1996]. *Q. calliprinos* is the dominant tree in
267 the Mediterranean scrub in Israel, while *Q. boissieri* grows mainly in altitudes above 500 m a.s.l
268 [Kaplan and Gutman, 1996]. The soil was formed on basaltic bedrock and is classified as Eutric
269 Lithosol in the FAO classification system and as Lithic Xerorthent in the USDA classification
270 system. The soil pH is 6.6 and the organic C content in the top 10 cm is 12% [Gross and Angert,
271 2017].

272 **2.2 Experimental design**

273 **2.2.1 Seasonal measurements**

274 Seasonal sampling took place in ten campaigns between February 2017 and May 2018. Soil air
275 was sampled from 1/2" (OD) stainless steel tubes closed at the bottom end, and perforated near
276 the bottom, that were hammered into the soil. The samples of soil air were collected from a depth
277 of 15 ± 4 cm in pre-evacuated ~ 3.6 mL glass flasks with Louwer™ O-ring high-vacuum valves.
278 Before sampling, the dead volume in the tubing and flask necks was purged with soil air by a

279 plastic syringe equipped with a two-way valve. A total of 120 samples were taken near each tree
280 species (2 replicates x 2 samples x 3 trees x 10 campaigns). Every tree was sampled only once
281 since sampling caused some disturbance to the soil and the stem (see below).

282 Surface soil from 0-10 cm depth was collected with a trowel and stored in a plastic bag.
283 A total of 30 samples were taken near each tree species by pooling from two places near each
284 tree (3 trees x 10 campaigns). Soil moisture was measured gravimetrically on ~3 g subsamples
285 (available only for the last 6 campaigns). For bulk soil incubation experiments, the soil was
286 sieved to 2 mm (except on January 2018 sampling when the soil was too wet and sticky to allow
287 sieving), and a subsample of 3 g was incubated overnight in 6 mL glass test tubes connected to
288 ~3.6 mL glass flasks by Ultra-Torr fittings (Swagelok, Solon, OH, USA). The gas in the
289 headspace had initial mean atmospheric values (20.95% O₂, 0.04% CO₂). Incubations were
290 conducted usually two days after soil collection at room temperature.

291 For estimating ARQ_{ts} we performed stem tissue incubations. This method was shown to
292 give similar ARQ values as the stem-chamber method in three species including the oak *Quercus*
293 *ilex* [Hilman et al., 2019]. We decided to incubate only the phloem and cambium tissues since
294 they are the most metabolically active tissues in the stem [Bowman et al., 2005], and since
295 transport in the phloem is the pathway for C to flow from the stem to the roots. Cores were
296 extracted using a 1.0 cm diameter cork borer, at 20 cm and 130 cm above the soil surface. A total
297 of 60 samples were taken from each tree species (2 stem positions x 3 trees x 10 campaigns). We
298 removed from the cores the outer bark and sapwood sieves, and further cut the cores to fit into
299 the 3.6 mL glass flask neck. For the incubations, we plugged the neck with a rubber stopper to
300 create a gas-tight headspace with initial mean atmospheric values. The incubations started
301 immediately after harvesting and lasted 3-4 hours in the dark and at environmental temperatures.
302 Metabolism in stem cores changes rapidly after harvesting; in a previous study ARQ_{ts} increased
303 with time after harvesting from 0.4 to values closer to 1.0 while the O₂ uptake rate was
304 maintained, indicating an increase in CO₂ efflux over time [Hilman et al., 2019]. The increased
305 ARQ_{ts} may provide evidence for gradual inhibition of PEPC activity that fixed respired CO₂
306 early during the incubation, but became less efficient as its own products accumulated. To
307 observe potential temporal changes in ARQ_{ts}, the tissues were re-incubated 24 hours after
308 harvesting (ARQ_{ts24}) for the same duration at room temperature. In the 24 h storage time stem
309 tissues were wrapped with moist gauze cloth to avoid desiccation.

310 2.2.2 Comparison of roots, bulk soil, and soil air ARQ and temperature effect

311 To evaluate the potential for ARQ to partition the contributions of autotrophic and heterotrophic
312 sources to total soil respiration, and to test the sensitivity of ARQ_{bs} to incubation temperature, we
313 sampled additional trees. During January 2019 we measured ARQ_{sa}, ARQ_{bs}, and ARQ_{root} near
314 three additional trees from each species. For ARQ_{root} fine roots (< 2 mm), which showed the
315 highest specific respiration rates among the root diameters tested, were excavated [Chen et al.,
316 2010; Desrochers et al., 2002; Pregitzer et al., 1998]. To test possible effects of root-surface
317 microbial communities on ARQ_{root}, soil was washed thoroughly from one subsample of roots
318 before incubation (n = 3), while a second subsample (n = 3) was incubated with the surrounding
319 soil. Roots were incubated shortly after harvesting in the dark in a set-up of two 3.6 mL glass
320 flasks connected by Ultra-Torr fitting, and kept at ~7°C to represent field condition (field soil
321 temperature was 6-8°C). Since we expected low respiration rates incubations lasted 24 h. We
322 also included in the comparison coarse roots of *Q. calliprinos* (< 1 cm in diameter) collected in

323 March 2018. Bulk soil incubations were conducted at temperatures of 6, 22, and 30 °C and lasted
 324 68-90 h (2 samples x 3 trees). The Q_{10} , the factor by which respiratory flux rises with a 10 °C
 325 increase, was calculated using the function Q_{10} from the R package *respirometry* [R Core Team,
 326 2019]. We also present ARQ_{bs} values for soils sampled in March and May 2018, when soil
 327 temperatures were 1°C and 22°C, respectively (n = 1).

328 **2.2.3 Evaluation of the effect of abiotic O₂ uptake on bulk soil ARQ**

329 Two additional soil incubation experiments were undertaken to investigate the potential for
 330 abiotic O₂ uptake to affect ARQ_{bs} . In the first experiment we tested the response to temporary
 331 anaerobic conditions with un-screened soils (for maintaining their structure). Mason jars (1 L)
 332 with a small volume of soil (~150 ml, n = 3) and jars with large soil volume (~550 ml, n = 3)
 333 were incubated for 13 days, to create low O₂ concentrations. Headspace [O₂] was measured by
 334 the end of the incubation, and soils were sampled for [Fe²⁺] and [Mn²⁺]. The soils were then
 335 ventilated for 1.5 hours, before an overnight incubation. Air and soil samples were measured
 336 again at the end of this incubation. The soil moisture measured at the beginning of the
 337 experiment was 31% by weight. The soil [Fe²⁺] was measured by the Ferrozine method [*Liptzin*
 338 *and Silver*, 2009]. The soil samples were sieved to 2 mm, and extracted by 0.5 M HCl
 339 immediately at the end of the incubation experiments. The soil [Mn²⁺] was measured by
 340 assuming that HCl-extractable Mn, which was quantified by ICP (7500cx Agilent technologies,
 341 Santa Clara, CA, USA), predominantly represents Mn²⁺ [*Keiluweit et al.*, 2018].

342 In a second experiment we tracked ARQ_{bs} during a wetting-drying cycle, and measured
 343 [Fe²⁺] and soil moisture during the soil drying. Ultra-Torr Tee fittings (Swagelok, Solon, OH,
 344 USA) were used for the incubation, connecting a test-tube with soil, a test-tube with a drying-
 345 agent (magnesium perchlorate), and a 3.6 ml flask equipped with Louwer™ O-ring high-vacuum
 346 valve. We incubated 2-mm sieved soil (n = 1) and un-sieved soil (n = 1). After every incubation
 347 the flask was closed and removed, the system was ventilated for 1 hour and then new flask was
 348 attached. The first incubation was used to determine the basal ARQ_{bs} and respiration rate (O₂
 349 uptake). The soil was then dried for 17 days, wetted, and dried again for 26 days. Soil wetting
 350 was roughly equivalent to a rainfall event of 20 mm. The destructive Fe²⁺ and soil moisture
 351 measurements during the soil drying were done for the sieved soil, after re-wetting it to the same
 352 degree. We report the relative respiration rate (RR) as the ratio between the O₂ uptake in each
 353 incubation to the basal rate.

354 **2.4 Gas analysis**

355 The [O₂] and [CO₂] of the air samples were measured in the laboratory by a closed system (The
 356 “*Hampadah*” [*Hilman et al.*, 2019]). The system is based on two analyzers: an infra-red gas
 357 analyzer (IRGA) for CO₂ measurement (LI 840A LI-COR; Lincoln, NE, USA) and a fuel-cell
 358 based analyzer (FC-10; Sable Systems International, Las Vegas, NV, USA) for measuring O₂,
 359 and is fully automated.

360 For measuring [CO₂] and [O₂] from the Mason jars we equipped each lid with a septum.
 361 Air from the headspace was sampled by plastic syringe with needle and injected into a flow-
 362 through CO₂ (K33 ICB 30% CO₂ Sensor, CO₂ Meter, Inc) and O₂ (Fibox 3, PreSens-Precision
 363 Sensing) sensors, connected by plastic tubing. The O₂ sensor is a quenching based optical fiber
 364 (optode) that reads the fluorescence from a sensing “spot”. We placed the “spot” in a 3 mm clear
 365 plastic aperture in an opaque lid of a custom-made 2-cm diameter flow-through cell, which made

366 from 4 mm thick aluminum base (to stabilized the temperature). From the outside of the aperture
 367 a connector for the optical fiber that reads the "spot" fluorescence was fixed. The same air was
 368 injected to pre-evacuated ~3.6 mL glass flasks for comparison with the "*Hampadah*" method.

369 **2.3 ARQ and respiratory fluxes estimations**

370 ARQ_{sa}, the CO₂ efflux/O₂ uptake in soil respiration, was calculated from the measured gases
 371 concertation using the following equation [Angert *et al.*, 2015]:

372
$$ARQ = \frac{D_{CO_2} \times ([CO_2]_s - [CO_2]_a)}{-D_{O_2} \times ([O_2]_s - [O_2]_a)} = -0.76 \times \frac{\Delta CO_2}{\Delta O_2} \quad (1)$$

373 Where D_{co2}, [CO₂]_s, and [CO₂]_a are respectively the effective diffusivity of gaseous CO₂,
 374 and the CO₂ concentrations in the soil (measured value) and in the ambient air (assumed to be
 375 0.04%). ΔCO₂ is therefore the difference in [CO₂] between the soil and the atmosphere. The
 376 same definitions hold for O₂, where the concentration in the ambient air assumed to be 20.95%.
 377 Since the O₂ flux is opposite in direction to the CO₂ flux we added negative sign for
 378 convenience. The effective diffusivity D depends on the structure of the pore spaces and on the
 379 diffusivity in air. It can be assumed that the structure is identical for CO₂ and O₂, therefore the
 380 ratio D_{co2}/ D_{o2} depends only on the CO₂/O₂ diffusivity ratio in air, which is 0.76 [Massman,
 381 1998].

382 Eq. 1 is somewhat analogous to the Davidson [Davidson, 1995] equation that estimates
 383 the respired δ¹³CO₂ in soil from soil-air discrete sample. The equation corrects for the faster
 384 diffusion of ¹²CO₂ (in our case O₂) that enriches the soil air with the slower-diffusing ¹³CO₂ (in
 385 our case CO₂), and for difference in δ¹³C and [CO₂] between the soil and the air above the soil.
 386 The Davidson equation accounts for diffusion and diffusive mixing and thus yields the same
 387 respired δ¹³CO₂ regardless soil depth [Bowling *et al.*, 2015; Egan *et al.*, 2019]. Eq. 1 is expected
 388 to similarly account for gas-mixing effects with depth [Angert *et al.*, 2015]. Indeed, ARQ_{sa} was
 389 similar when measured at depths of 10, 30, and 60 cm (0.3, [Sanchez-Canete *et al.*, 2018]) and at
 390 30 and 90 cm (0.8, [Hicks Pries *et al.*, 2019]). Moreover, as ΔCO₂ and ΔO₂ are calculated with
 391 respect to atmospheric air, advective mixing of soil air with the above air is not expected to
 392 change the measured ARQ_{sa}. Nonetheless, since such mixing will violate the diffusional steady-
 393 state between different soil depths we avoided sampling in days with high wind speeds (> 4 m s⁻¹).
 394

395 ARQ_{bs}, ARQ_{ts}, and ARQ_{ts24} were calculated by the ratio between [CO₂] and [O₂] net
 396 percent changes in the incubation headspace. ARQ_{bs} values were further corrected for CO₂
 397 dissolution since the large volume of water in the bulk soil samples collected during winter and
 398 the fairly high pH value for non-calcareous soil (6.6) are expected to cause to some of the
 399 respired CO₂ to convert into DIC. DIC (mmol/L), the sum of dissolved CO₂, H₂CO₃, HCO₃⁻, and
 400 CO₃²⁻, was calculated using Eq. 2 [Stumm and Morgan, 1996]:

401
$$DIC = P_{CO_2} \times k_h \times \left(1 + \frac{k_1}{10^{-pH}} + \frac{k_1 \times k_2}{(10^{-pH})^2} \right) \quad (2)$$

402 where P_{CO2} is the partial pressure of gaseous CO₂ (= [CO₂]/100), k_h is Henry's constant
 403 that states the amount of dissolved CO₂ and H₂CO₃ in the water, and k₁ and k₂ are the first and
 404 second acidity constants, respectively. The constants are temperature dependent and calculated
 405 according to the incubation temperature [Harned and Davis, 1943; Harned and Scholes Jr,
 406 1941]. To estimate the addition of DIC during incubation we assumed the initial DIC was in

407 equilibrium with atmospheric [CO₂] of 0.04%, and the final DIC in equilibrium with the final
 408 [CO₂]. The net change in the calculated DIC (ΔDIC) was converted to gaseous CO₂ equivalent
 409 and added to the measured [CO₂]_{measured}, yielding the corrected [CO₂]_c:

$$410 \quad [CO_2]_c = [CO_2]_{measured} + 100 \times \frac{\Delta DIC \times W \times 22.4}{V_{HS}} \quad (3)$$

411 where W is the absolute amount of water in the sample (L) and V_{HS} is the headspace
 412 volume (mL). When soil moisture data were unavailable, we estimated its value from the relation
 413 between the available soil moisture data and rainfall in the last 3 weeks. The term 22.4 converts
 414 the units of the dissolved CO₂ (mmol) to mL gas.

415 The O₂ uptake and CO₂ efflux from the bulk-soil incubations were calculated using the
 416 equation (nanomole gas g.DW⁻¹ min⁻¹):

$$417 \quad Flux = \frac{\Delta Gas \times V_{HS} \times BP}{t \times M \times I_t \times 8.314 \times 10^{-3}} \quad (4)$$

418 where ΔGas is net percent change in the gas concentration ([O₂] or [CO₂]) during the
 419 incubation, BP is the local barometric pressure (hPa), t is the temperature (k), M is the soil dry
 420 weight (g), I_t is the incubation time (min), and 8.314 × 10⁻³ is the ideal gas constant (mL hPa k⁻¹
 421 nanomol⁻¹). Soil samples were oven-dried (105°C, 24 h) for dry weights.

422 **2.5 Statistical analysis**

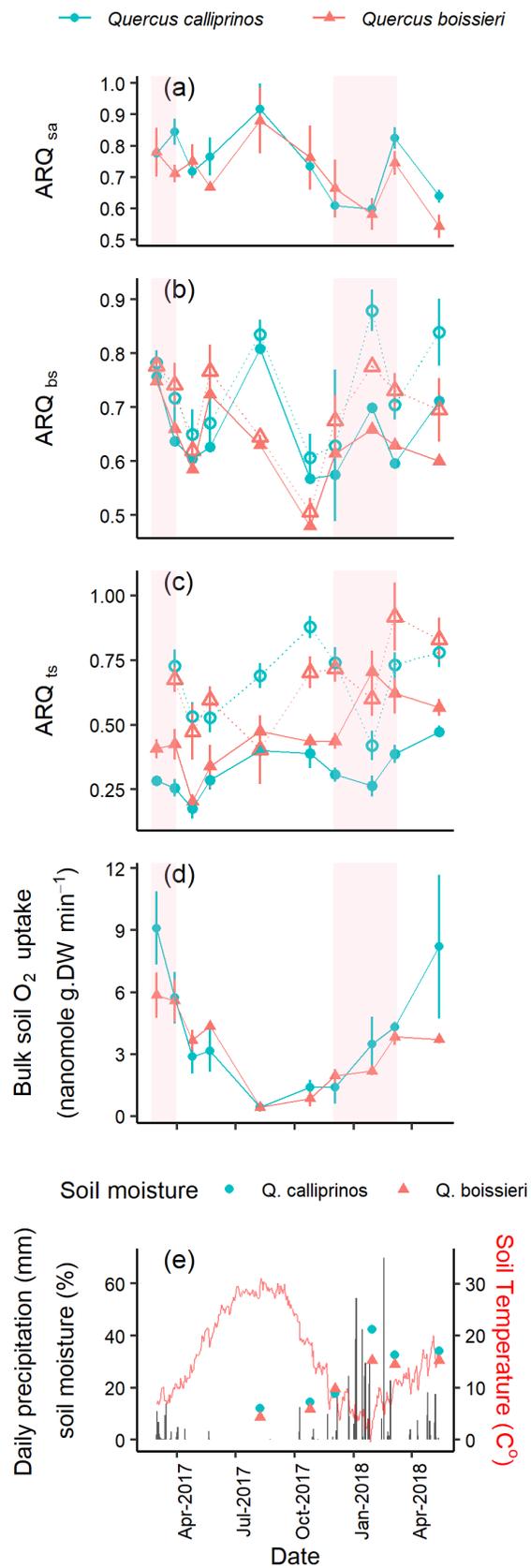
423 All comparisons were conducted using one-way analysis of variance (ANOVA) and a *t*-test, after
 424 assuring homogeneity of variances using Bartlett's test. For unequal variances we used a
 425 Welch's test and nonparametric comparisons with Wilcoxon method. Significant differences
 426 were determined at *P* < 0.05. The relations of the seasonal ARQ and bulk-soil O₂ uptake values
 427 with physical parameters were tested using backward selection technique for multiple
 428 regressions, including estimates of the interactions between each two factors. The tested
 429 parameters were: soil moisture (available for the last 6 out of 10 campaigns), the number of days
 430 passed since the last rain event, the accumulated rain in the 3 weeks prior to sampling, and soil
 431 temperature at 10 cm depth. Rainfall and temperature were measured in the nearby metrological
 432 station of El rom (data courtesy of Meteo-Tech Ltd. Meteorological Services). We used linear
 433 regressions not only to evaluate the relationship of dependent and independent variables, but also
 434 to describe correlation between ARQ_{ts} and ARQ_{sa}. All statistical analysis was done using JMP
 435 (JMP®, JMP Pro 13, SAS Institute Inc., Cary, NC, USA).

436 **3 Results**

437 **3.1 Seasonal measurements**

438 The seasonal ARQ measurements are presented in Figure 2. The overall mean ± SE values
 439 (range of means per species per date) of ARQ_{sa}, ARQ_{bs} (without correction for CO₂ dissolution
 440 in water), ARQ_{ts}, and ARQ_{ts24} were respectively 0.76 ± 0.02 (0.60-0.92), 0.65 ± 0.02 (0.47-0.80),
 441 0.39 ± 0.03 (0.19-0.70), and 0.68 ± 0.04 (0.42-1.08). The dissolution correction for ARQ_{bs} values
 442 increased the mean value and range to 0.72 (0.51-0.88). The correction had some sensitivity to
 443 the parameters pH, W (soil water content), and V_{HS} (incubation headspace) (Eq. 2-3). The
 444 decrease of V_{HS} in 10%, and the increase of W in 10% and the pH from 6.6 to 6.8 resulted in an
 445 increase of the overall mean to 0.76. Varying the parameters in the same magnitude but in

446 opposite direction yielded overall mean of 0.69. The weighted mean of the corrected ARQ_{bs}
447 (using O₂ uptake rates for weighting) further increased the mean value to 0.75 (0.53-0.90). From
448 this point on in the paper ARQ_{bs} values will refer to values corrected for CO₂ dissolution.
449 Significant difference between species were observed only in ARQ_{ts} ($P = 0.0015$, *Welch* test,
450 both stem heights pooled together) with mean values of 0.46 ± 0.03 and 0.32 ± 0.02 for *Q.*
451 *boissieri* and *Q. calliprinos*, respectively. Marginal significance ($P = 0.06$, *t* test) was observed
452 for the weighted ARQ_{bs} where *Q. calliprinos* was higher than *Q. boissieri* (0.77 vs. 0.72).



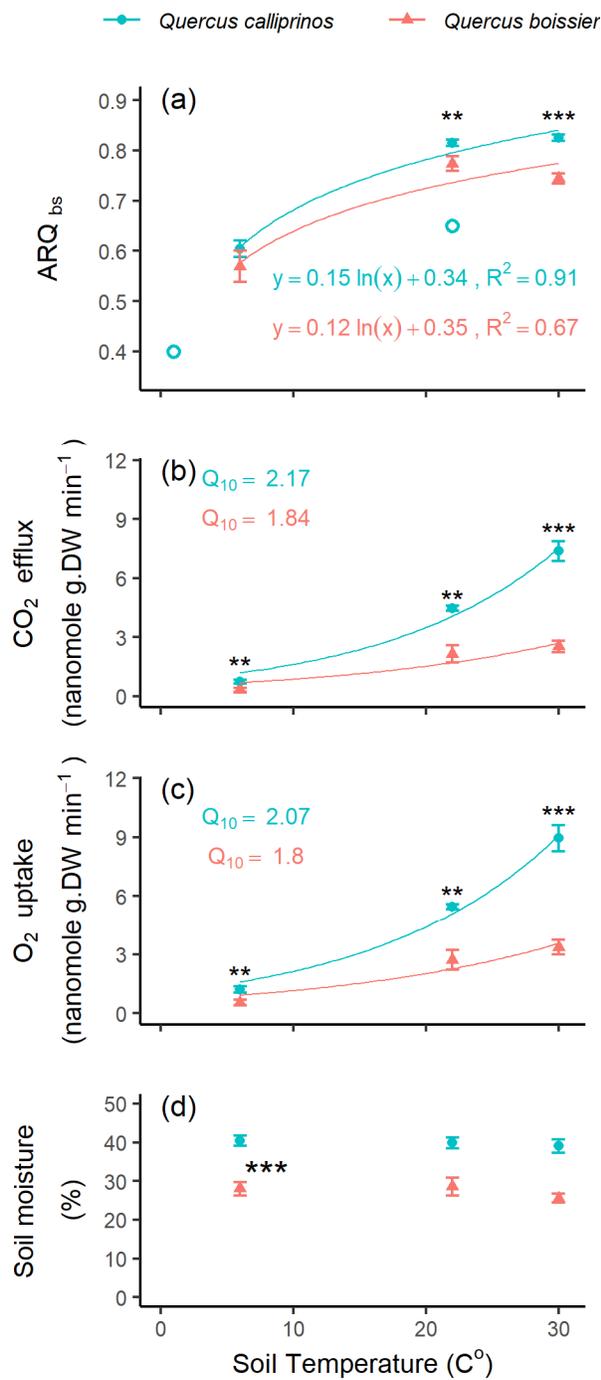
454 Figure 2. Seasonal measurements of (a) $ARQ_{sa} \pm SE$, the ratio of CO_2 efflux/ O_2 uptake measured
 455 for soil air in depth of 15 ± 4 cm ($n = 3$); (b) ARQ measured from bulk soil incubation (ARQ_{bs})
 456 where full markers with soil line indicate the measured values and empty markers with dashed
 457 lines indicate the dissolution corrected values ($n = 3$); (c) the mean ARQ measured for incubated
 458 stem tissues (ARQ_{ts}) extracted from at 20 and 130 cm above the ground (ARQ_{ts} , full markers
 459 indicate incubations conducted directly after the core was harvested; empty markers with dashed
 460 lines indicate incubations conducted 24 h after harvest) sampled 20 and 130 cm above ground,
 461 (d) the O_2 uptake rate of the incubated bulk soils, (e) daily precipitation (black bars) and soil
 462 temperature (blue line) measured by adjacent meteorological station and the soil moisture in the
 463 site. Shaded periods indicate winter dormancy of the deciduous *Q. boissieri*. Soil sampling was
 464 conducted underneath the trees. Error bars represents standard errors.

465 3.2 Bulk soil measurements

466 The seasonal variability of ARQ_{bs} was not explained by the tested physical parameters in the
 467 backward selection technique. When temperature was tested individually it had positive effect on
 468 ARQ_{bs} between 1-6 and 22°C, while between 22 and 30°C ARQ_{bs} values were rather stable (Fig.
 469 3a). At the highest temperatures we observed species effect with higher values in the *Q.*
 470 *calliprinos* (Fig.3a). The *Q. calliprinos* also had higher CO_2 and O_2 fluxes, greater sensitivity to
 471 temperature (higher Q_{10} values, Fig. 3b,c), and greater soil moisture than the *Q. boissieri* (Fig.
 472 3d). For correction of the seasonal incubations conducted at room temperature to field soil
 473 temperature, we used a logarithmic fit ($R^2 = 0.78$) equation for the relation between $T_{incubation}$ (the
 474 temperature in which the incubation took place (C°)) and ARQ_{bs} for both species:

$$475 \quad ARQ_{bs} = 0.13 \times \ln(T_{incubation}) + 0.36 \quad (5)$$

476



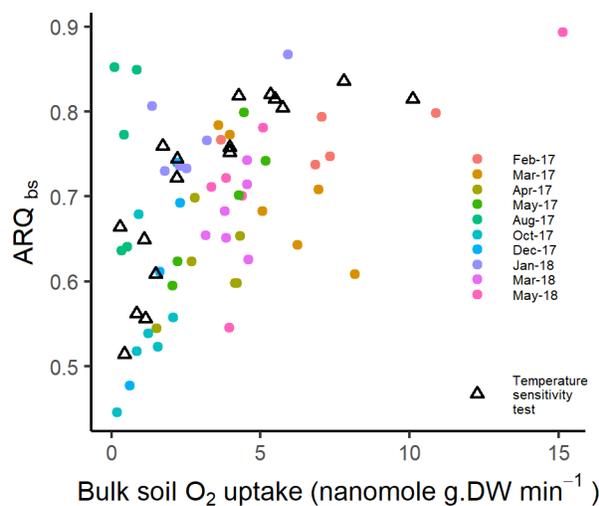
477
 478 Figure 3. Results (mean \pm SE) from bulk soil incubations at different temperatures. Filled
 479 symbols represent soils collected on January 2019 underneath three trees from each species with
 480 two soil samples per tree ($n=6$). Empty symbols represent soils collected on March and May
 481 2018. (a) ARQ_{bs} (ratio of CO₂ efflux/O₂ uptake) with logarithmic fit, (b) the CO₂ efflux rates
 482 (after CO₂ dissolution correction) and the calculated temperature coefficient Q₁₀, (c) the O₂
 483 uptake rates and the calculated Q₁₀ values, and (d) the gravimetric moisture of the soils.
 484 Asterisks indicate significance difference between species (** - $P < 0.01$, *** - $P < 0.001$) in t

485 test, expect for the CO₂ and O₂ fluxes at 22°C where Welch test was used. For soil moisture
 486 comparison was made for all temperatures together.

487 A trend of higher ARQ_{bs} values with higher bulk-soil O₂ uptake rates was observed for
 488 both the seasonal measurements and the temperature-controlled incubations (Fig. 4). In addition,
 489 variability declined with increasing O₂ uptake rates. The bulk-soil O₂ uptake rate showed a
 490 strong seasonal cycle, with maximal uptake rates during spring (March-May) and minimal rates
 491 during the end of the summer (August-October) (Fig. 2d). The uptake rates of the two species did
 492 not differ significantly ($P = 0.766$, t test). A reciprocal effect on bulk-soil O₂ uptake rate
 493 (nanomole O₂ g.DW min⁻¹) was found between soil moisture (M) and soil temperature (T_{soil}).
 494 The effect is described by the following equation:

$$495 \quad \text{O}_2 \text{ uptake} = 17.50 M + 0.09 T_{\text{soil}} + (T - 14.5) \times (M - 0.24) \times 0.59 - 2.79 \quad (6)$$

496 The actual respiration rate versus the equation predicted respiration gives $R^2 = 0.94$ ($P <$
 497 0.0001). A significant linear relation was found also between bulk-soil O₂ uptake and the number
 498 of days elapsed since the last rain event ($R^2 = 0.4$, $P = 0.005$). Adding this effect to the prediction
 499 formula does not improve R^2 which remains 0.94 (no reciprocal effect was found in relation to
 500 this parameter). A correlation coefficient R^2 of 0.75 ($P < 0.001$) was calculated while assuming
 501 M is the only driving factor on bulk-soil O₂ uptake.
 502



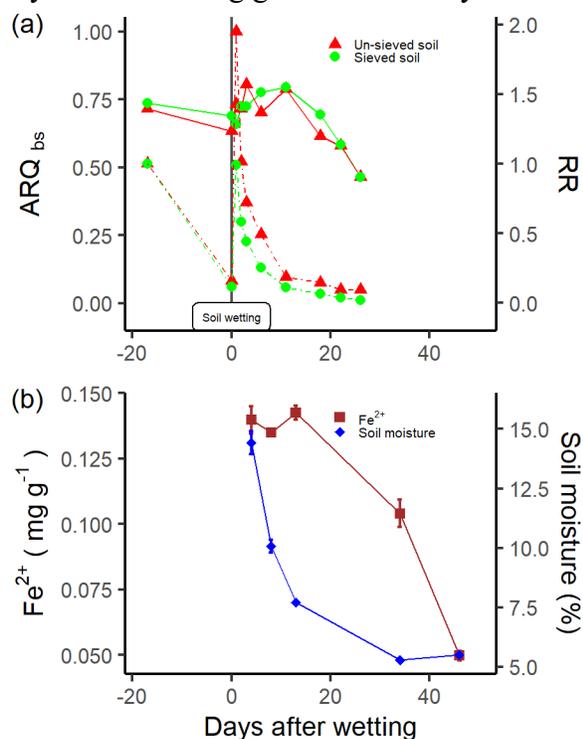
503
 504 Figure 4. Scatter plot of ARQ (the ratio of CO₂ efflux/O₂ uptake) measured from bulk soil
 505 incubations (ARQ_{bs}) and the O₂ uptake rate of the incubated bulk soils. Results are grouped by
 506 the month of sampling for the seasonal measurements (colored circles) and temperature

507 3.2.1 Relation between ARQ_{bs} and Fe²⁺

508 After the first 13-days of incubation the average [O₂] ± SD of the incubation jars with the large
 509 and small soil volumes were 0.90 ± 0.44% and 7.25 ± 0.07%, respectively (n = 3). In agreement,
 510 [Fe²⁺] in the jars with large soil volume was higher than measured for the small soil volume jars
 511 (0.89 ± 0.24 vs. 0.05 ± 0.01 mg g⁻¹ soil, respectively). In the subsequent incubation, performed
 512 after ventilation of 1.5 hours aimed to increase the [O₂] in the jars, a sharp decrease in [O₂] was
 513 observed in the large soil volume jars from an ambient value of 20.95% to value of 4.77 ±

514 0.21%, while ARQ was 0.37 ± 0.01 . The $[\text{Fe}^{2+}]$ dropped from 0.89 ± 0.24 to $0.21 \pm 0.04 \text{ mg g}^{-1}$
 515 soil. The $[\text{Mn}^{2+}]$ was 1.27 mg g^{-1} soil, and did not significantly change during this incubation. In
 516 the small soil volume jars the $[\text{O}_2]$ decreased from 20.95% to $19.80 \pm 0.26\%$, ARQ was
 517 0.74 ± 0.02 , and $[\text{Fe}^{2+}]$ did not change from the initial value of 0.05 mg g^{-1} soil. Taking into
 518 account the different soil volumes, the rate of O_2 uptake was 2.9-fold faster in the large soil
 519 volume jars than in the small soil volume jars. The $[\text{CO}_2]$ and $[\text{O}_2]$ determined by the sensors in
 520 this experiment were highly consistent with the *Hampadah* measurement (R^2 of 0.997 and 0.975
 521 in linear regression with slopes of 1.01 and 1.01, respectively).

522 The soil wetting-drying experiment induced variations in ARQ_{bs} , RR, and $[\text{Fe}^{2+}]$ (Fig. 5).
 523 RR peaked in the day of soil wetting and then gradually decreased. Following the soil wetting
 524 ARQ_{bs} increased during 11 days from 0.63-0.69 to 0.79-0.80 and then decreased during 15 days
 525 to 0.46. $[\text{Fe}^{2+}]$ values of $\sim 0.14 \text{ mg g}^{-1}$ were measured during the first 13 days after soil wetting, at
 526 soil moisture values of 14.4%-7.7%. After the 13th day $[\text{Fe}^{2+}]$ decreased to 0.10 mg g^{-1} in the 34th
 527 day and to 0.05 mg g^{-1} in the 46th day.



528 Figure 5. Results from soil drying-rewetting experiment. The day of the rewetting is day 0. (a)
 529 ARQ_{bs} (ratio of CO_2 efflux/ O_2 uptake) in solid lines and relative respiration rate (RR) in dashed
 530 lines for un-sieved and sieved (2 mm) soils. Each data point represents one measurement without
 531 replicates. (b) The concentration of Fe^{2+} (mg g^{-1}) and the gravimetric moisture of the sieved soil.
 532 Following the experiment presented in panel a, the same sieved soil was wetted to the same
 533 moisture. Each data point represents mean of duplicate sub-samples taken from the drying soil.
 534 Error bars are the standard deviations.
 535

536 3.3 Soil air measurements

537 Concentrations of CO_2 and O_2 in the soils in single tube samplings ranged from 0.17 - 2.25% and
 538 20.79 - 18.14%, respectively. The lowest O_2 concentrations were measured during January 2018

539 after 163 mm of precipitation over the previous 3 weeks. The seasonal variability of ARQ_{sa} was
 540 explained by the water related parameters M , the number of days passed since the last rain event
 541 (D), and accumulated rain in the 3 weeks prior to sampling (R) in the backward selection
 542 technique. A reciprocal effect was found between the last two factors. The statistical model is
 543 defined by the equation:

$$544 \quad ARQ_{sa} = 0.47M + 0.02D + 0.004R + (D - 18) \times (R - 58.5) \times 3 \times 10^{-4} + 0.24 \quad (7)$$

545 With $P = 0.0002$ on F test and the correlation between the actual and predicted soil ARQ
 546 gives R^2 of 0.94. The effect of T_{soil} is small testing all-year time scale and its addition to the
 547 prediction formula has a minor contribution to the coefficient of determination. However, when
 548 omitting from the analysis data collected during late winter and spring and including only data
 549 from May 2017 – Jan 2018, ARQ_{sa} is found to be strongly dependent in temperature ($R^2 = 0.92$,
 550 $P < 0.0001$). The relation is given by the linear equation: $ARQ_{sa} = 0.01 \times T_{soil} + 0.6$.

551 **3.4 Comparison of ARQ in bulk soil, roots, and soil air**

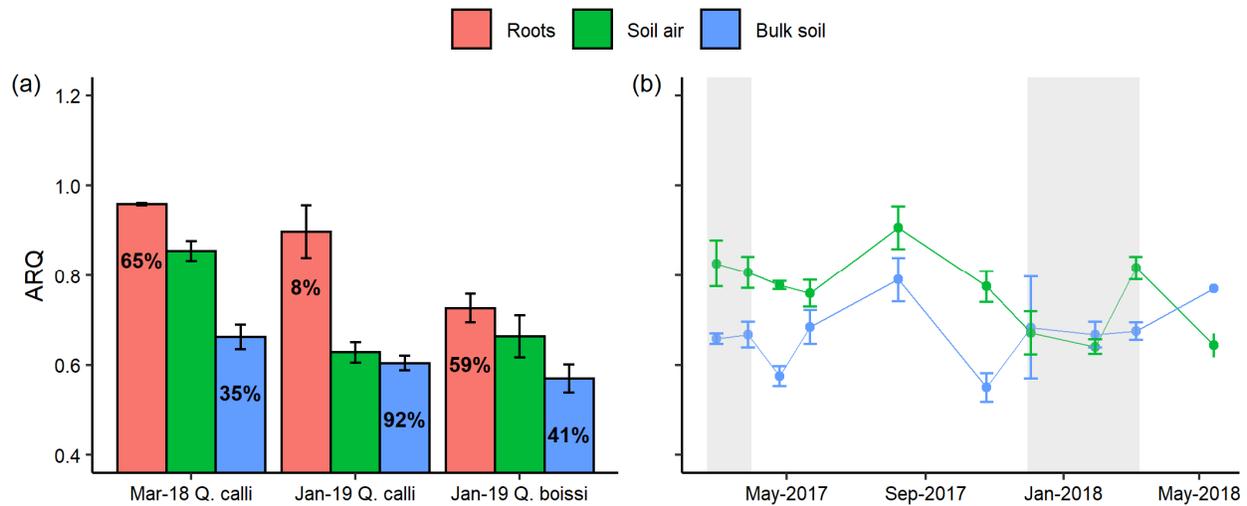
552 The mean ARQ_{root} per species per date ranged between 0.73-0.96 (Fig 6a). The root washing
 553 treatment in roots collected in January 2019 did not affect ARQ_{root} ($P = 0.99$, t test) therefore
 554 results were pooled together. ARQ_{sa} values were always lower than ARQ_{root} and higher than
 555 ARQ_{bs} (Fig. 6a). Assuming root and bulk-soil respiration are the only end members affecting the
 556 soil pore space air, their relative contributions could be estimated using a simple mixing model,
 557 where $ARQ_{sa} = X \times ARQ_{root} + (1 - X) \times ARQ_{bs}$ (Fig. 6a).

558 The seasonal ARQ_{bs} measurements were conducted in room temperature and not in the
 559 actual field soil temperature. Thus, for comparison of ARQ_{bs} and ARQ_{sa} (measured at field
 560 conditions) ARQ_{bs} has to be corrected to field temperature. We first averaged values of both
 561 species at each measurement date. Then the intercept term b from Eq. 5 was modified:

$$562 \quad b = 0.36 - (ARQ_{t=room} - ARQ_{bs_measured}) \quad (8)$$

563 Where 0.36 is the calculated intercept as appears in Eq. 5, $ARQ_{t=room}$ is the expected
 564 ARQ according to Eq. 5 and the room temperature (varied slightly between measurements), and
 565 $ARQ_{bs_measured}$ is the measured ARQ in the bulk-soil incubation, corrected to CO_2 dissolution.
 566 The bulk soil ARQ values reported in Figure 7b were calculated with the equation:

$$567 \quad ARQ = 0.13 \times \ln(T_{soil}) + b \quad (9)$$



568 Figure 6. (a) A comparison of ARQ (ratio of CO₂ efflux/O₂ uptake) values (mean ± SE)
 569 measured from root incubations (n = 2, 6, 6), soil air (n = 3), and bulk-soil incubations (n = 3).
 570 The x axis indicates the date of sampling and the tree species. The relative contributions (%) of
 571 roots and bulk-soil respiration to the total soil respiration are indicated in the bars. The
 572 contributions were calculated using the equation $ARQ_{sa} = X \times ARQ_{root} + (1 - X) \times ARQ_{bs}$. (b)
 573 The seasonal course of ARQ means (± SE, n = 6) of both tree species, where the bulk soil values
 574 are temperature corrected according to Eq. 9. Shaded periods indicate winter dormancy of the
 575 deciduous *Q. boissieri*.
 576

577

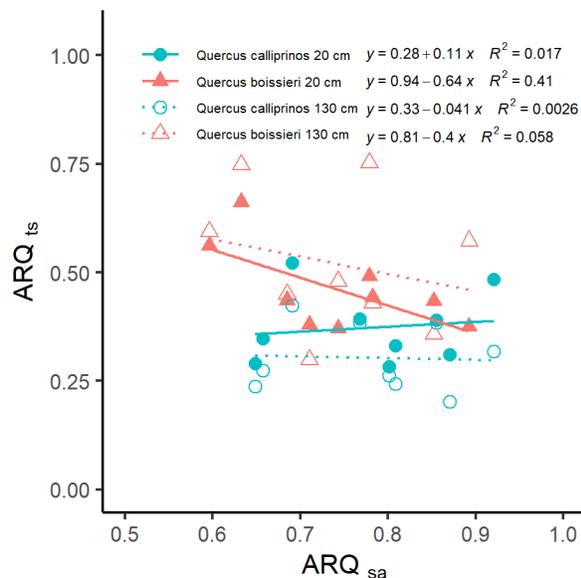
578 3.5 Tree stem measurements

579 The strongest effect on ARQ measured in tree stems was time; ARQ_{ts} values measured in
 580 incubations started immediately after tissues extraction were much lower than ARQ_{ts24} measured
 581 in incubation started 24 h after the extraction (Fig. 2c). The overall ARQ_{ts} and ARQ_{ts24} means
 582 (±SE) for the *Q. boissieri* were 0.46 ± 0.03 and 0.68 ± 0.03 , respectively ($P < 0.0001$, Welch
 583 test), and for the *Q. calliprinos* 0.32 ± 0.02 and 0.67 ± 0.03 , respectively ($P < 0.0001$, Welch
 584 test). The sampling height of the stem cores (20 and 130 cm) had no significant effect when
 585 analyzed separately for ARQ_{ts} and ARQ_{ts24} in both species ($P = 0.14$ at the minimum).

586 In general, the deciduous *Q. boissieri* exhibited greater seasonal variability than the
 587 evergreen *Q. calliprinos*. The *Q. boissieri* ARQ_{ts} values during winter exfoliation were
 588 significantly higher than the *Q. calliprinos* (0.51 ± 0.02 vs. 0.30 ± 0.02 , $P < 0.0001$, Welch
 589 test), while during the foliated period higher *Q. boissieri* values were not significant (0.41 ± 0.03 vs.
 590 0.34 ± 0.03 , $P = 0.11$, *t* test). In contrast, the species did not differ in their ARQ_{ts24} values ($P =$
 591 0.66 , *t* test) also during winter exfoliation ($P = 0.07$, Welch test).

592 The seasonal variability of the *Q. boissieri* was explained by physical factors in the
 593 backward selection technique. The most effective factor was the accumulated rain in the 3 weeks
 594 prior to sampling for ARQ_{ts} ($R^2 = 0.85$, $P < 0.001$) and for ARQ_{ts24} ($R^2 = 0.93$, $P < 0.001$). Soil
 595 moisture was also correlated with ARQ_{ts} ($R^2 = 0.71$, $P = 0.04$) and with ARQ_{ts24} ($R^2 = 0.82$,
 596 $P = 0.03$). One outlier point was excluded in each correlation. For the *Q. calliprinos* no

597 correlation was found. Inverse correlation with marginal significance was found between the *Q.*
 598 *boissieri* ARQ_{ts} at 20 cm above the ground and ARQ_{sa} ($R^2 = 0.41$, $P = 0.06$) after excluding 1
 599 outlier point out of 10 (measured in April 2017 when ARQ_{ts} was minimal, Fig. 3).



600
 601 Figure 7. Scatter plot of stem ARQ (ratio of CO₂ efflux/O₂ influx) measured from incubated
 602 stem cores containing phloem and cambium tissues (ARQ_{ts}) sampled 20 (filled symbols) and 130
 603 cm (hollow symbols) above ground from the main trunks of the tree species *Quercus calliprinos*
 604 and *Quercus boissieri*, against soil air ARQ measured below the same trees. Each point
 605 represents the mean value of three trees (stems and underlying soils) measured in each campaign.
 606 The *P* values of the correlations are 0.7393, 0.0618, 0.8973, and 0.533 ordered as appears in the
 607 legend.

608 **4 Discussion**

609 In the first part of the discussion we interpret the results of the current study. The second part is
 610 dedicated to discussion about methodology and future research towards more meaningful use of
 611 ARQ in soil and ecosystem studies.

612 **4.1 Bulk-soil ARQ results indicate the respiratory substrate is more reduced than**
 613 **mean SOC**

614 The overall weighted mean of the dissolution-corrected ARQ_{bs} is 0.75, well within the range of
 615 previous ARQ_{bs} assessments (Fig. 1) and similar to values of 0.75-0.80 measured in different
 616 natural soils in Germany [Dilly, 2001; 2003; Dilly and Zyakun, 2008]. An ARQ_{bs} value of 0.75 is
 617 appreciably below 0.95, the ARQ_{bs} expected by SOM-C_{ox} median value in soils meta-analysis
 618 study, and slightly below 0.77, the lowest expected value [Worrall et al., 2013]. Several potential
 619 processes can be ruled out as drivers for the low weighted mean ARQ_{bs}, including dissolution of
 620 respired CO₂ in the soil water (after the dissolution correction) and reversible effects such O₂
 621 uptake by oxidizing Fe²⁺ or Mn²⁺ that should be canceled by anaerobic respiration that must
 622 occur at different time in the soil (e.g. to reduce Fe and Mn). However, other processes with
 623 potentially irreversible effects, including microbial re-fixation of respired CO₂ and oxidative
 624 depolymerization are both possible explanations.

625 Studies of CO₂ ‘dark’ fixation showed that rates scaled with microbial biomass regardless
626 of soil depth [Akinyede *et al.*, 2020]; thus we speculate that a constant fraction of respired CO₂ is
627 re-fixed regardless the season. If the re-fixation products, which are usually relatively oxidized,
628 are mineralized shortly after synthesis, no net effect on ARQ is to be expected. However, if the
629 re-fixed C persists in microbial biomass or SOM, there will be a net decrease in ARQ.
630 Nonetheless, the effect is small and accounting for the highest observed re-fixation rates (5.6%;
631 [Akinyede *et al.*, 2020]), only slightly increases our ARQ_{bs} mean, to 0.79.

632 Oxidative depolymerization breaks down macromolecules by introduction of oxygen-rich
633 groups, which forms small molecules that microbes can uptake easily. The polymer oxidation
634 step consumes O₂ and is expected to lower ARQ_{bs}. However, the mineralization of the highly
635 oxygenated produced molecules is expected to have high ARQ_{bs}, with overall a zero net effect on
636 ARQ_{bs}. Net reduction of ARQ_{bs} might occur if the oxygen-rich molecules escape microbial
637 digestion and associate with minerals, where an extended time period may pass until their
638 mineralization [Kleber *et al.*, 2015]. We estimate that in natural soils the fraction of C
639 associating to mineral surface is very small comparing to overall mineralization rates, thus the
640 net effect of oxidative depolymerization on ARQ_{bs} should be small. We therefore conclude the
641 mean ARQ_{bs} of 0.75 mainly reflects the stoichiometry of the respiratory substrate.

642 The difference between the expected ARQ_{bs} value according to the apparent SOM-C_{ox}
643 and the measured ARQ_{bs} suggests that the overall SOM is more oxidized than the smaller SOM
644 pool that is more accessible to microbes and directly supports respiration. Since oxidized
645 compounds are energetically more labile than reduced compounds (Table 1) the plethora of low
646 ARQ_{bs} results indicate that C_{ox} alone is insufficient to predict the decomposability of soil
647 compounds. The C_{ox} difference between the respiratory substrate and the total SOM is similar to
648 radiocarbon measurements where bulk-soil respired CO₂ is much younger than the total SOM
649 [Trumbore, 2000], which suggests most SOM has slow turnover rates with small contribution to
650 respiration. Hence, rather than representing the total SOM stoichiometry, ARQ_{bs} provides
651 information about the C_{ox} of the actual labile pool utilized by microbes.

652 ARQ_{bs} values lower than expected based on the bulk-SOM composition also indicates an
653 oxidation of the remaining, unrespired SOM (unless the C influx to the SOM has exactly same
654 C_{ox} as the respired C). This consequence is expected regardless the reason for the low ARQ_{bs}. If
655 reduced compounds with smaller O content are decomposed preferentially, the remainder SOM
656 is becoming more enriched with oxidized molecules. Same net effect is expected if the low
657 ARQ_{bs} is due to excess of bulk-soil O₂ uptake. This expectation is in line with observed SOM
658 oxidation trends over longer time scales. For example, Rock-Eval indices show increases in C_{ox}
659 (higher oxygen index and lower hydrogen index) with soil depth [Sebag *et al.*, 2016], with aging
660 of bare fallow [Barré *et al.*, 2016], and with experimental soil warming [Poeplau *et al.*, 2019].
661 Free-air CO₂ enrichment experiment (FACE) experiments also resulted in increased C_{ox} values in
662 SOM after nine years of elevated CO₂ treatment [Hockaday *et al.*, 2015]. The oxidation was
663 explained by a loss of reduced lipids and lignin and increased abundance of oxidized carbonyl
664 groups. Using the change in the C stocks, the authors further calculated the net respiration fluxes
665 accompanying the C_{ox} change (OR = 1.477), would be equivalent to an ARQ of 0.68, which is
666 similar to our mean ARQ_{bs} value of 0.75.

667 4.2 Fe²⁺ redox changes affect ARQ_{bs} only at low respiration rates

668 ARQ_{bs} values were associated with respiration (i.e. O₂ uptake) rate, which varied by two orders
 669 of magnitude in our experiments (Fig. 4, 5a). At respiration rates above ~3 nanomole O₂ g.DW⁻¹
 670 min⁻¹ most ARQ_{bs} values were similar to the mean weighted seasonal value (0.7-0.8) with
 671 relatively small variability, while during lower respiration rates larger ARQ_{bs} variability were
 672 observed (0.4-0.9; Fig. 4). One possible explanation for this observation is greater sensitivity of
 673 the O₂ measurement for smaller O₂ fluxes. However, the low ARQ_{bs} values measured at low
 674 temperatures (Fig. 3) and in the soil drying experiment (Fig. 5a) seem like part of a trend and not
 675 just arbitrary analytical noise. Alternatively, the ARQ_{bs} and O₂ uptake relation can be explained
 676 by a shift in the dominant processes. When respiration rates are low, slower processes (i.e. those
 677 normally contributing only in a minor way to larger O₂ fluxes), such as oxidative
 678 depolymerization and redox related changes in Fe, can have a measurable effect on ARQ_{bs}. As
 679 respiration rates increase the ARQ_{bs} value related to substrate-stoichiometry will drown out other
 680 effects.

681 In the jar incubations with soils recovering from anaerobic conditions ([O₂] ~1%) the
 682 ARQ_{bs} was 0.37 and [Fe²⁺] decreased sharply. The stoichiometry for the overall oxidation of
 683 Fe²⁺ ions by O₂, O_{2(aq)} + 4Fe²⁺ + 6H₂O ↔ 4FeOOH_(s) + 8H⁺ [Burke and Banwart, 2002],
 684 explains 27% of the drop in [O₂], another third of the O₂ uptake can be explained by faster
 685 oxidation of soil organic matter that usually follows anaerobic conditions (e.g. [Keiluweit et al.,
 686 2017]), while the last third can be explained by the same microbial respiration as in the control
 687 soils. For comparison, the initial [O₂] in the control jars was ~7% and the subsequent ARQ_{bs} was
 688 0.74 with no change in [Fe²⁺]. As the air in the anaerobic treatment was nearly anoxic, the ARQ_{bs}
 689 difference between 0.74 and 0.37 seems to represent the maximal effect of Fe²⁺ oxidation for the
 690 site. However, the soil drying-rewetting experiment indicates Fe redox change has only a small
 691 influence under field conditions (Fig. 5). The decrease in ARQ_{bs} values on the 11th day after soil
 692 wetting seems to be the result of Fe²⁺ oxidation that occurred around the same time – by this time
 693 point, respiration rates were already low. We estimated that the amount of O₂ decrease due to
 694 Fe²⁺ oxidation, which is equivalent to the amount of alternative oxidants during anaerobic
 695 respiration, is less than 10% of the O₂ flux when respiration rates were higher. In addition, the
 696 minimal [O₂] measured in the soil air was 18.14% therefore anoxia might present only in
 697 microsites and not in the whole soil profile. Moreover, the fast [O₂] transition from ~1% to
 698 20.95% in the jar incubations that resulted the sharp ARQ_{bs} decrease is not expected in the field.
 699 Gradual [O₂] increase with smaller effect on ARQ_{bs} is rather expected. Thus, we conclude that
 700 redox-related O₂ consumption is significant at Odem forest only at low respiration rates.

701 4.3 Seasonality of soil air ARQ indicates soil respiration is controlled by bulk-soil 702 respiration

703 The overall mean ARQ_{sa} was 0.76, within the range of previous studies (Fig. 1). ARQ_{sa} was
 704 almost always higher than ARQ_{bs} and when ARQ_{root} was measured its values exceeded ARQ_{sa},
 705 apparently confirming that ARQ_{sa} value is the weighted mean of those two end members and that
 706 ARQ can be used for partitioning of soil respiration sources (Fig. 6). Our results further support
 707 the view that variability in ARQ_{sa} reflects shifting dominance between root and microbially-
 708 mediated heterotrophic respiration sources [Hicks Pries et al., 2019].

709 The backward selection technique indicates that on a yearly basis water-related
 710 parameters are the main factors controlling the seasonal ARQ_{sa} variability in this Mediterranean

711 site, with negligible effect of T_{soil} (Fig. 2a; Eq. 7). With two orders of magnitude variability, the
 712 bulk-soil O_2 uptake rate (at room temperature) was also mainly controlled by soil moisture (Fig
 713 2d; Eq. 6). We lack information about the seasonal variability of root respiration rates, but based
 714 on other studies in Mediterranean climates, it can be assumed the rate from tree roots is rather
 715 constant [Tang and Baldocchi, 2005; Vose and Ryan, 2002]. We therefore estimate that in Odem
 716 forest ARQ_{sa} is mainly controlled by variability in ARQ_{bs} , which in turn mainly controlled by
 717 soil moisture. T_{soil} was important factor with positive effect on ARQ_{sa} only outside the high
 718 growth period (May to January) when soil respiration rates were slow (Fig. 2). A similar positive
 719 effect of T_{soil} on ARQ_{sa} was observed at 30 cm depth in heated soils (+4°C) during winter [Hicks
 720 Pries *et al.*, 2019]. This trend is in accordance with the effect of temperature on ARQ_{bs} ; a
 721 positive effect when respiration rates are slow, and no effect when respiration rates are high (Fig.
 722 3, 4).

723 Deviations of ARQ_{sa} from ARQ_{bs} and ARQ_{root} values might resulted from soil profile
 724 processes that might be present in the field and not in the ARQ_{bs} and ARQ_{root} incubations. For
 725 example, CO_2 that otherwise would be released to the soil air might dissolve in the soil water and
 726 leach. This process can explain the few ARQ_{sa} values that were equal to or lower than ARQ_{bs}
 727 during the second and wetter winter (Fig. 2, 6). In contrast if the soil water does not leach the
 728 dissolved CO_2 can degasses back to the pore space after water evaporation or warming that
 729 reduces CO_2 solubility. Such degassing could explain the spike in ARQ_{sa} observed during the
 730 last campaign of the second winter (Fig 6). In the area of Odem forest only 10-30% of annual
 731 precipitation (950 mm) leaches to groundwater [Dafny *et al.*, 2006], most of it during episodic
 732 intensive rain events during winter. Therefore we estimate the loss of respired CO_2 to
 733 groundwater is negligible on an annual basis, though it might affect specific sampling dates.

734 4.4 Tree stems ARQ

735 The ARQ values measured in tree stem tissues were considerably lower than 1.0, the value
 736 expected from carbohydrate respiration (Table 1) in most plants [Hoch *et al.*, 2003; Plaxton and
 737 Podestá, 2007]. The mean ARQ_{ts} and $\text{ARQ}_{\text{ts}24}$ values were 0.39 and 0.68, respectively. Damage
 738 during the tissue extraction from the stems might result in a burst of O_2 uptake that lowered
 739 ARQ_{ts} values. One indication for such a short-term wound response on O_2 uptake is elevated
 740 H_2O_2 production observed within two hours after epicormic shoot wounding [Tian *et al.*, 2015].
 741 Therefore, $\text{ARQ}_{\text{ts}24}$ (measured 24 h after tissues extraction) can be considered as less prone to
 742 artifacts, although metabolic change during the 24 h period is possible [Hilman *et al.*, 2019]. The
 743 $\text{ARQ}_{\text{ts}24}$ mean values of ~ 0.7 could be explained by pure lipid substrates for respiration (Table
 744 1). This is, however, not expected, especially in the tree genera *Quercus* [Hoch *et al.*, 2003;
 745 Sinnott, 1918]. The current results thus reinforce our recent studies and suggest that tree stem
 746 ARQ do not merely reflect the substrate's stoichiometry and additional non-respiratory effects
 747 are at work [Angert *et al.*, 2012; Hilman *et al.*, 2019].

748 Our observations indicate differences between the species that are related to phenology.
 749 During the foliated period of the deciduous *Q. boissieri* its ARQ_{ts} was similar to the evergreen *Q.*
 750 *calliprinos* values, however during winter exfoliation the *Q. boissieri* values increased in ~ 0.2
 751 ARQ units above the *Q. calliprinos* values (Fig. 2). The seasonal change of ARQ_{ts} and $\text{ARQ}_{\text{ts}24}$
 752 of the *Q. boissieri* were explained by water related factors suggesting low tree stem ARQ is
 753 associated with dry conditions. We speculated that if re-fixation of respired CO_2 by the enzyme
 754 PEPC is the process that lowers tree-stems ARQ, the enzyme's products like the organic acids

755 citrate and malate might be exported via the phloem to the roots and be secreted to the soil as
 756 root exudates [*Hoffland et al.*, 2006; *Shane et al.*, 2004]. In agreement, a recent study in a
 757 different Mediterranean forest in Israel reported that root exudation rates were highest in the dry
 758 season and were associated with high soil temperature and low soil moisture [*Jakoby et al.*,
 759 2020]. Indeed, the inverse relationship between ARQ_{ts} vs. ARQ_{sa} at 20 cm in the deciduous *Q.*
 760 *boissieri* (Fig. 7) might suggest catabolism of organic acids, with high ARQ in the soil offsetting
 761 low stem ARQ (Table 1). However the *Q. calliprinos* ARQ_{ts} values were rather uniform
 762 throughout the year without correlation with ARQ_{sa} . The fact that ARQ_{sa} of both species had
 763 almost the same seasonal changes suggests that the variability in ARQ_{sa} is not related to ARQ_{ts} .
 764 It is highly probable that our tube sampling from depth of ~15 cm, used to estimate ARQ_{sa} , did
 765 not fully capture the autotrophic signal of shallow fine roots. Section 4.5.2 adds more discussion
 766 about this topic.

767 **4.5 What should be done next?**

768 In this section we discuss future research of ARQ in soils. Suggested future steps in tree stem
 769 ARQ research are discussed at [*Hilman et al.*, 2019].

770 **4.5.1 Bulk-soil incubations**

771 For estimating ARQ_{bs} we measured the change of $[CO_2]$ and $[O_2]$ in the headspace of closed-
 772 system incubations. We further corrected for CO_2 dissolution in the soil moisture, especially due
 773 to the relatively basic pH value (6.6) and large amount of soil water per headspace volume. A
 774 way to reduce the amount of dissolved CO_2 is by increasing the incubation set-up. With fixed
 775 soil water content, increasing the ratio incubation headspace/ soil mass by a given factor would
 776 decrease the amount of dissolved CO_2 by the same factor.

777 We conclude that when respiration rates are high, the ARQ_{bs} signal mostly reflects the
 778 substrate stoichiometry of microbial respiration. One way to test this would be to amend soil
 779 incubations with compounds differing in their expected ARQ, for example lipids or soluble
 780 amino acids with $ARQ < 1$, sugars with $ARQ = 1$, and organic-acids with $ARQ > 1$. Ideally the
 781 compounds should have different $\delta^{13}C$ signatures than the SOM to allow calculation of the
 782 contribution of the amended compound to the respired C. Previously, addition of sugars (with
 783 $ARQ = 1$) to bulk-soil incubations indeed resulted in higher ARQ_{bs} compared to basal values of
 784 0.8, but the resulting ARQ values varied between 0.95 and 1.6 and depended on the added
 785 amount of sugar and the sampling timing after the amendment [*Dilly and Zyakun*, 2008]. High
 786 amounts of added substrate caused a ‘priming effect’ that rapidly altered microbial composition
 787 and metabolism, thus the resulting ARQ does not represent purely the stoichiometry of the
 788 amendment. We therefore suggest amending soils with smaller amounts of ^{13}C -labeled substrate
 789 to better mimic natural input rates. The role of oxidative depolymerization and CO_2 re-fixation in
 790 ARQ_{bs} variability can be tested by parallel measurement of ARQ_{bs} and the activity of oxidases
 791 (enzymes that use O to break-down large molecules) and rates of CO_2 re-fixation.

792 Temperature was found to have an effect on ARQ_{bs} . Moisture effects were not tested
 793 separately, but the higher ARQ_{bs} at 22 and 30°C in *Q. calliprinos* compared to *Q. boissieri* soils
 794 may reflect the higher soil moisture in the *Q. calliprinos* (Fig. 3). Higher water content can affect
 795 ARQ_{bs} via faster respiration (similarly to the discussed temperature effect), or via faster diffusion
 796 of dissolved organic C that can fuel microbial respiration with different substrates. Better
 797 understanding of these effects can also improve ARQ_{bs} predictions with seasonal changes.

798 Therefore factorial incubations in different temperatures and soil moistures to test these effects
799 separately are recommended.

800 **4.5.2 Total soil ARQ and partitioning respiration sources**

801 As mentioned in the introduction, the very few available soil-chamber-ARQ_{sa} measurements
802 yielded higher values than estimated from gas profiles and diffusion modeling. The assumed
803 reason is that the soil chamber better captures the signal of processes like respiration from fine
804 roots (with high ARQ) that are usually concentrated in soil horizons above the ones sampled by
805 gas probes (e.g. [Claus and George, 2005]). Under-representation of the shallow roots might
806 explain the lack of the expected inverse stem-soil respiration ARQ relations. The influence of
807 surface litter decomposition is another process not represented in gas diffusion models. Hence, to
808 evaluate the contribution of soil respiration ARQ to the total ecosystems ARQ balance requires
809 surface chamber measurements to at least compare with gas tube/diffusion estimates. However,
810 measurement of ARQ using tube sampling is easier than chamber sampling since the O₂ signals
811 are larger and easier to detect, and the sampling is fast and simple technically. Comparing both
812 measurements is expected to yield interesting results, especially testing the assumptions that are
813 presented in Section 2.3 and Eq. 1, and to make a sensitivity test to find under which conditions
814 (e.g. advective mixing) Eq. 1 becomes invalid.

815 ARQ has the potential to partition the sources of soil respiration. In comparison to other
816 non-destructive methods like the bomb-radiocarbon approach and canopy $\delta^{13}\text{C}$ -labeling the use
817 of ARQ can be technically simpler and more cost-effective [Kuznyakov, 2006]. There are few
818 considerations that yet should be taken: different ARQ_{bs} signals from soils sampled from
819 different depths, their temporal variability, and their relative contributions to the total respiration
820 fluxes.

821 **Acknowledgments**

822 We thank Goni Shachar for helping with field work, Maayan Farbman for helping in soil
823 incubations, Joe Von Fischer for valuable discussion, and Susan Trumbore for critical reading.
824 This research was supported by the Israel Science Foundation (grant # 773/19), and by the
825 German–Israeli Foundation for Scientific Research and Development (no. 1334/2016). The data
826 are available in <https://figshare.com/s/db7b0e2c5b5dfbcb28bf>.

827 **References**

- 828 Akinyede, R., M. Taubert, M. Schrumpf, S. Trumbore, and K. Küsel (2020), Rates of dark CO₂
829 fixation are driven by microbial biomass in a temperate forest soil, *Soil Biology and*
830 *Biochemistry*, *150*, 107950.
- 831 Angert, A., J. Muhr, R. Negron Juarez, W. Alegria Muñoz, G. Kraemer, J. Ramirez Santillan, E.
832 Barkan, S. Mazeh, J. Q. Chambers, and S. E. Trumbore (2012), Internal respiration of Amazon
833 tree stems greatly exceeds external CO₂ efflux, *Biogeosciences*, *9*(12), 4979–4991,
834 doi:10.5194/bg-9-4979-2012.
- 835 Angert, A., and Y. Sherer (2011), Determining the relationship between tree-stem respiration and
836 CO₂ efflux by $\delta\text{O}_2/\text{Ar}$ measurements, *Rapid Commun Mass Spectrom*, *25*(12), 1752–1756,
837 doi:10.1002/rcm.5042.

- 838 Angert, A., D. Yakir, M. Rodeghiero, Y. Preisler, E. Davidson, and T. Weiner (2015), Using O₂
839 to study the relationships between soil CO₂ efflux and soil respiration, *Biogeosciences*, *12*(7),
840 2089-2099.
- 841 Aon, M. A., D. E. Sarena, J. L. Burgos, and S. Cortassa (2001a), Interaction between gas
842 exchange rates, physical and microbiological properties in soils recently subjected to agriculture,
843 *Soil and Tillage Research*, *60*(3-4), 163-171, doi:10.1016/s0167-1987(01)00191-x.
- 844 Aon, M. A., D. E. Sarena, J. L. Burgos, and S. Cortassa (2001b), (Micro)biological, chemical
845 and physical properties of soils subjected to conventional or no-till management: an assessment
846 of their quality status, *Soil and Tillage Research*, *60*(3-4), 173-186, doi:10.1016/s0167-
847 1987(01)00190-8.
- 848 Aubrey, D. P., and R. O. Teskey (2009), Root-derived CO₂ efflux via xylem stream rivals soil
849 CO₂ efflux, *New Phytol*, *184*(1), 35-40, doi:10.1111/j.1469-8137.2009.02971.x.
- 850 Bais, H. P., T. L. Weir, L. G. Perry, S. Gilroy, and J. M. Vivanco (2006), The role of root
851 exudates in rhizosphere interactions with plants and other organisms, in *Annual Review of Plant*
852 *Biology*, edited, pp. 233-266, Annual Reviews, Palo Alto,
853 doi:doi:10.1146/annurev.arplant.57.032905.105159.
- 854 Barré, P., et al. (2016), The energetic and chemical signatures of persistent soil organic matter,
855 *Biogeochemistry*, *130*(1-2), 1-12, doi:10.1007/s10533-016-0246-0.
- 856 Battle, M. O., et al. (2019), Atmospheric measurements of the terrestrial O₂ : CO₂ exchange ratio
857 of a midlatitude forest, *Atmospheric Chemistry and Physics*, *19*(13), 8687-8701,
858 doi:10.5194/acp-19-8687-2019.
- 859 Benavente, J., I. Vadillo, F. Carrasco, A. Soler, C. Liñán, and F. Moral (2010), Air Carbon
860 Dioxide Contents in the Vadose Zone of a Mediterranean Karst, *Vadose Zone Journal*, *9*(1), 126-
861 136, doi:10.2136/vzj2009.0027.
- 862 Berveiller, D., and C. Damesin (2007), Carbon assimilation by tree stems: potential involvement
863 of phosphoenolpyruvate carboxylase, *Trees*, *22*(2), 149-157, doi:10.1007/s00468-007-0193-4.
- 864 Berveiller, D., J. Vidal, J. Degrouard, F. Ambard-Bretteville, J. N. Pierre, D. Jaillard, and C.
865 Damesin (2007), Tree stem phosphoenolpyruvate carboxylase (PEPC): lack of biochemical and
866 localization evidence for a C₄-like photosynthesis system, *New Phytol*, *176*(4), 775-781,
867 doi:10.1111/j.1469-8137.2007.02283.x.
- 868 Bloemen, J., M. A. McGuire, D. P. Aubrey, R. O. Teskey, and K. Steppe (2013), Transport of
869 root-respired CO₂ via the transpiration stream affects aboveground carbon assimilation and
870 CO₂ efflux in trees, *New Phytol*, *197*(2), 555-565, doi:10.1111/j.1469-8137.2012.04366.x.
- 871 Bloom, A. J., R. M. Caldwell, J. Finazzo, R. L. Warner, and J. Weissbart (1989), Oxygen and
872 carbon dioxide fluxes from barley shoots depend on nitrate assimilation, *Plant Physiol*, *91*(1),
873 352-356, doi:10.1104/pp.91.1.352.
- 874 Bowling, D. R., J. E. Egan, S. J. Hall, and D. A. Risk (2015), Environmental forcing does not
875 induce diel or synoptic variation in the carbon isotope content of forest soil respiration,
876 *Biogeosciences*, *12*(16), 5143-5160, doi:10.5194/bg-12-5143-2015.
- 877 Bowman, W. P., M. M. Barbour, M. H. Turnbull, D. T. Tissue, D. Whitehead, and K. L. Griffin
878 (2005), Sap flow rates and sapwood density are critical factors in within- and between-tree

- 879 variation in CO₂ efflux from stems of mature *Dacrydium cupressinum* trees, *New Phytol*, 167(3),
880 815-828, doi:10.1111/j.1469-8137.2005.01478.x.
- 881 Burke, S. P., and S. A. Banwart (2002), A geochemical model for removal of iron(II)(aq) from
882 mine water discharges, *Applied Geochemistry*, 17(4), 431-443, doi:10.1016/s0883-
883 2927(01)00092-0.
- 884 Chen, D., L. Zhou, X. Rao, Y. Lin, and S. Fu (2010), Effects of root diameter and root nitrogen
885 concentration on in situ root respiration among different seasons and tree species, *Ecological*
886 *Research*, 25(5), 983-993, doi:10.1007/s11284-010-0722-2.
- 887 Claus, A., and E. George (2005), Effect of stand age on fine-root biomass and biomass
888 distribution in three European forest chronosequences, *Canadian Journal of Forest Research*,
889 35(7), 1617-1625, doi:10.1139/x05-079.
- 890 Cuezva, S., A. Fernandez-Cortes, D. Benavente, P. Serrano-Ortiz, A. S. Kowalski, and S.
891 Sanchez-Moral (2011), Short-term CO₂(g) exchange between a shallow karstic cavity and the
892 external atmosphere during summer: Role of the surface soil layer, *Atmospheric Environment*,
893 45(7), 1418-1427, doi:10.1016/j.atmosenv.2010.12.023.
- 894 Dafny, E., A. Burg, and H. Gvirtzman (2006), Deduction of groundwater flow regime in a
895 basaltic aquifer using geochemical and isotopic data: The Golan Heights, Israel case study,
896 *Journal of Hydrology*, 330(3-4), 506-524, doi:10.1016/j.jhydrol.2006.04.002.
- 897 Davidson, G. R. (1995), The Stable Isotopic Composition and Measurement of Carbon in Soil
898 CO₂, *Geochimica Et Cosmochimica Acta*, 59(12), 2485-2489, doi:Doi 10.1016/0016-
899 7037(95)00143-3.
- 900 De Vries, F. W. T. P., A. H. M. Brunsting, and H. H. Van Laar (1974), Products, requirements
901 and efficiency of biosynthesis a quantitative approach, *Journal of Theoretical Biology*, 45(2),
902 339-377, doi:10.1016/0022-5193(74)90119-2.
- 903 Desrochers, A., S. M. Landhausser, and V. J. Lieffers (2002), Coarse and fine root respiration in
904 aspen (*Populus tremuloides*), *Tree Physiol*, 22(10), 725-732, doi:10.1093/treephys/22.10.725.
- 905 Dilly, O. (2001), Microbial respiratory quotient during basal metabolism and after glucose
906 amendment in soils and litter, *Soil Biology and Biochemistry*, 33(1), 117-127,
907 doi:10.1016/s0038-0717(00)00123-1.
- 908 Dilly, O. (2003), Regulation of the respiratory quotient of soil microbiota by availability of
909 nutrients, *FEMS Microbiol Ecol*, 43(3), 375-381, doi:10.1111/j.1574-6941.2003.tb01078.x.
- 910 Dilly, O., and A. Zyakun (2008), Priming Effect and Respiratory Quotient in a Forest Soil
911 Amended with Glucose, *Geomicrobiology Journal*, 25(7-8), 425-431,
912 doi:10.1080/01490450802403099.
- 913 Druschel, G. K., D. Emerson, R. Sutka, P. Suchecki, and G. W. Luther (2008), Low-oxygen and
914 chemical kinetic constraints on the geochemical niche of neutrophilic iron(II) oxidizing
915 microorganisms, *Geochimica et Cosmochimica Acta*, 72(14), 3358-3370,
916 doi:10.1016/j.gca.2008.04.035.
- 917 Egan, J. E., D. R. Bowling, and D. A. Risk (2019), Technical Note: Isotopic corrections for the
918 radiocarbon composition of CO₂ in the soil gas environment must account for diffusion and
919 diffusive mixing, *Biogeosciences*, 16(16), 3197-3205, doi:10.5194/bg-16-3197-2019.

- 920 Emmerich, W. E. (2003), Carbon dioxide fluxes in a semiarid environment with high carbonate
921 soils, *Agricultural and Forest Meteorology*, *116*(1-2), 91-102, doi:10.1016/s0168-
922 1923(02)00231-9.
- 923 Gallagher, M. E., F. L. Liljestrand, W. C. Hockaday, and C. A. Masiello (2017), Plant species,
924 not climate, controls aboveground biomass O₂:CO₂ exchange ratios in deciduous and coniferous
925 ecosystems, *J Geophys Res-Biogeophys*, *122*(9), 2314-2324, doi:10.1002/2017jg003847.
- 926 Gallagher, T. M., and D. O. Breecker (2020), The Obscuring Effects of Calcite Dissolution and
927 Formation on Quantifying Soil Respiration, *Global Biogeochemical Cycles*, *34*(12),
928 e2020GB006584, doi:ARTN e2020GB006584
929 10.1029/2020GB006584.
- 930 Gross, A., and A. Angert (2017), Use of ¹³C- and phosphate ¹⁸O-labeled substrate for studying
931 phosphorus and carbon cycling in soils: a proof of concept, *Rapid Commun Mass Sp*, *31*(11),
932 969-977.
- 933 Grossiord, C., L. Mareschal, and D. Epron (2012), Transpiration alters the contribution of
934 autotrophic and heterotrophic components of soil CO₂ efflux, *New Phytol*, *194*(3), 647-653,
935 doi:10.1111/j.1469-8137.2012.04102.x.
- 936 Hall, S. J., and W. L. Silver (2013), Iron oxidation stimulates organic matter decomposition in
937 humid tropical forest soils, *Glob Chang Biol*, *19*(9), 2804-2813, doi:10.1111/gcb.12229.
- 938 Harned, H. S., and R. Davis (1943), The ionization constant of carbonic acid in water and the
939 solubility of carbon dioxide in water and aqueous salt solutions from 0 to 50 degrees, *Journal of*
940 *the American Chemical Society*, *65*(10), 2030-2037, doi:DOI 10.1021/ja01250a059.
- 941 Harned, H. S., and S. R. Scholes Jr (1941), The ionization constant of HCO₃⁻ from 0 to 50,
942 *Journal of the American Chemical Society*, *63*(6), 1706-1709.
- 943 Hawkins, H.-J., M. D. Cramer, and E. George (1999), Root respiratory quotient and nitrate
944 uptake in hydroponically grown non-mycorrhizal and mycorrhizal wheat, *Mycorrhiza*, *9*(1), 57-
945 60.
- 946 Hibberd, J. M., and W. P. Quick (2002), Characteristics of C₄ photosynthesis in stems and
947 petioles of C₃ flowering plants, *Nature*, *415*(6870), 451-454, doi:10.1038/415451a.
- 948 Hicks Pries, C., A. Angert, C. Castanha, B. Hilman, and M. S. Torn (2019), Using Respiration
949 Quotients to Track Changing Sources of Soil Respiration Seasonally and with Experimental
950 Warming, *Biogeosciences Discuss.*, *2019*, 1-20, doi:10.5194/bg-2019-232.
- 951 Hilman, B., et al. (2019), Comparison of CO₂ and O₂ fluxes demonstrate retention of respired
952 CO₂ in tree stems from a range of tree species, *Biogeosciences*, *16*(1), 177-191, doi:10.5194/bg-
953 16-177-2019.
- 954 Hoch, G., A. Richter, and C. Korner (2003), Non-structural carbon compounds in temperate
955 forest trees, *Plant, Cell and Environment*, *26*(7), 1067-1081, doi:10.1046/j.0016-
956 8025.2003.01032.x.
- 957 Hockaday, W. C., M. E. Gallagher, C. A. Masiello, J. A. Baldock, C. M. Iversen, and R. J. Norby
958 (2015), Forest soil carbon oxidation state and oxidative ratio responses to elevated CO₂, *Journal*
959 *of Geophysical Research-Biogeosciences*, *120*(9), 1797-1811, doi:10.1002/2015jg003010.

- 960 Hoffland, E., R. Boogaard, J. Nelemans, and G. Findenegg (2006), Biosynthesis and root
 961 exudation of citric and malic acids in phosphate-starved rape plants, *New Phytologist*, *122*(4),
 962 675-680, doi:[10.1111/j.1469-8137.1992.tb00096.x](https://doi.org/10.1111/j.1469-8137.1992.tb00096.x).
- 963 Hoffland, E., R. Van Den Boogaard, J. Nelemans, and G. Findenegg (1992), Biosynthesis and
 964 root exudation of citric and malic acids in phosphate-starved rape plants, *New Phytologist*,
 965 *122*(4), 675-680, doi:<https://doi.org/10.1111/j.1469-8137.1992.tb00096.x>.
- 966 Ishidoya, S., S. Murayama, C. Takamura, H. Kondo, N. Saigusa, D. Goto, S. Morimoto, N. Aoki,
 967 S. Aoki, and T. Nakazawa (2013), O₂: CO₂ exchange ratios observed in a cool temperate
 968 deciduous forest ecosystem of central Japan, *Tellus B: Chemical and Physical Meteorology*,
 969 *65*(1), 21120.
- 970 Jakoby, G., I. Rog, S. Megidish, and T. Klein (2020), Enhanced root exudation of mature
 971 broadleaf and conifer trees in a Mediterranean forest during the dry season, *Tree Physiol*, *40*(11),
 972 1595-1605, doi:[10.1093/treephys/tpaa092](https://doi.org/10.1093/treephys/tpaa092).
- 973 Kaplan, D., and M. Gutman (1996), Effect of Thinning and Grazing on Tree Development and
 974 the Visual Aspect of an Oak Forest on the Golan Heights, *Israel Journal of Plant Sciences*,
 975 *44*(4), 381-386, doi:[10.1080/07929978.1996.10676659](https://doi.org/10.1080/07929978.1996.10676659).
- 976 Keeling, R. F. (1988), Development of an interferometric oxygen analyzer for precise
 977 measurement of the atmospheric O₂ mole fraction, Harvard University, Cambridge,
 978 Massachusetts.
- 979 Keiluweit, M., K. Gee, A. Denney, and S. Fendorf (2018), Anoxic microsites in upland soils
 980 dominantly controlled by clay content, *Soil Biology and Biochemistry*, *118*, 42-50,
 981 doi:[10.1016/j.soilbio.2017.12.002](https://doi.org/10.1016/j.soilbio.2017.12.002).
- 982 Keiluweit, M., T. Wanzek, M. Kleber, P. Nico, and S. Fendorf (2017), Anaerobic microsites
 983 have an unaccounted role in soil carbon stabilization, *Nature communications*, *8*(1), 1771.
- 984 Kleber, M., K. Eusterhues, M. Keiluweit, C. Mikutta, R. Mikutta, and P. S. Nico (2015),
 985 Mineral–organic associations: formation, properties, and relevance in soil environments, in
 986 *Advances in agronomy*, edited, pp. 1-140, Elsevier.
- 987 Kuzyakov, Y. (2006), Sources of CO₂ efflux from soil and review of partitioning methods, *Soil*
 988 *Biology and Biochemistry*, *38*(3), 425-448, doi:<https://doi.org/10.1016/j.soilbio.2005.08.020>.
- 989 Lambers, H., F. S. Chapin, and T. L. Pons (2008), Respiration, in *Plant Physiological Ecology*,
 990 edited, pp. 101-150, Springer New York, New York, NY, doi:[10.1007/978-0-387-78341-3_3](https://doi.org/10.1007/978-0-387-78341-3_3).
- 991 LaRowe, D. E., and P. Van Cappellen (2011), Degradation of natural organic matter: a
 992 thermodynamic analysis, *Geochimica et Cosmochimica Acta*, *75*(8), 2030-2042.
- 993 Liptzin, D., and W. L. Silver (2009), Effects of carbon additions on iron reduction and
 994 phosphorus availability in a humid tropical forest soil, *Soil Biology and Biochemistry*, *41*(8),
 995 1696-1702.
- 996 Ma, J., Z. Y. Wang, B. A. Stevenson, X. J. Zheng, and Y. Li (2013), An inorganic CO₂ diffusion
 997 and dissolution process explains negative CO₂ fluxes in saline/alkaline soils, *Sci Rep*, *3*, 2025,
 998 doi:[10.1038/srep02025](https://doi.org/10.1038/srep02025).

- 999 Masiello, C. A., M. E. Gallagher, J. T. Randerson, R. M. Deco, and O. A. Chadwick (2008),
1000 Evaluating two experimental approaches for measuring ecosystem carbon oxidation state and
1001 oxidative ratio, *Journal of Geophysical Research*, *113*(G3), doi:10.1029/2007jg000534.
- 1002 Massman, W. J. (1998), A review of the molecular diffusivities of H₂O, CO₂, CH₄, CO, O₃, SO₂,
1003 NH₃, N₂O, NO, and NO₂ in air, O₂ and N₂ near STP, *Atmospheric Environment*, *32*(6), 1111-
1004 1127, doi:10.1016/s1352-2310(97)00391-9.
- 1005 Miltner, A., F. D. Kopinke, R. Kindler, D. E. Selesi, A. Hartmann, and M. Kastner (2005), Non-
1006 phototrophic CO₂ fixation by soil microorganisms, *Plant and Soil*, *269*(1-2), 193-203,
1007 doi:10.1007/s11104-004-0483-1.
- 1008 Plaxton, W. C., and F. E. Podestá (2007), The Functional Organization and Control of Plant
1009 Respiration, *Critical Reviews in Plant Sciences*, *25*(2), 159-198,
1010 doi:10.1080/07352680600563876.
- 1011 Poeplau, C., P. Barré, L. Cécillon, F. Baudin, and B. D. Sigurdsson (2019), Changes in the Rock-
1012 Eval signature of soil organic carbon upon extreme soil warming and chemical oxidation-A
1013 comparison, *Geoderma*, *337*, 181-190.
- 1014 Pregitzer, K. S., M. J. Laskowski, A. J. Burton, V. C. Lessard, and D. R. Zak (1998), Variation in
1015 sugar maple root respiration with root diameter and soil depth, *Tree Physiol*, *18*(10), 665-670,
1016 doi:10.1093/treephys/18.10.665.
- 1017 R Core Team (2019), R: A Language and Environment for Statistical Computing, edited.
- 1018 Rachmilevitch, S., H. Lambers, and B. Huang (2006), Root respiratory characteristics associated
1019 with plant adaptation to high soil temperature for geothermal and turf-type *Agrostis* species, *J*
1020 *Exp Bot*, *57*(3), 623-631, doi:10.1093/jxb/erj047.
- 1021 Sanchez-Canete, E. P., G. A. Barron-Gafford, and J. Chorover (2018), A considerable fraction of
1022 soil-respired CO₂ is not emitted directly to the atmosphere, *Sci Rep*, *8*(1), 13518,
1023 doi:10.1038/s41598-018-29803-x.
- 1024 Schill, V., W. Hartung, B. Orthen, and M. H. Weisenseel (1996), The xylem sap of maple (*Acer*
1025 *platanoides*) trees—sap obtained by a novel method shows changes with season and height,
1026 *Journal of Experimental Botany*, *47*(1), 123-133, doi:10.1093/jxb/47.1.123.
- 1027 Sebag, D., et al. (2016), Dynamics of soil organic matter based on new Rock-Eval indices,
1028 *Geoderma*, *284*, 185-203, doi:10.1016/j.geoderma.2016.08.025.
- 1029 Seibt, U., W. A. Brand, M. Heimann, J. Lloyd, J. P. Severinghaus, and L. Wingate (2004),
1030 Observations of O₂:CO₂ exchange ratios during ecosystem gas exchange, *Global*
1031 *Biogeochemical Cycles*, *18*(4), n/a-n/a, doi:10.1029/2004gb002242.
- 1032 Severinghaus, J. P. (1995), Studies of the terrestrial O₂ and carbon cycles in sand dune gases and
1033 in biosphere 2, Columbia University.
- 1034 Sexstone, A. J., N. P. Revsbech, T. B. Parkin, and J. M. Tiedje (1985), Direct measurement of
1035 oxygen profiles and denitrification rates in soil aggregates, *Soil science society of America*
1036 *journal*, *49*(3), 645-651.
- 1037 Shane, M. W., M. D. Cramer, S. Funayama-Noguchi, G. R. Cawthray, A. H. Millar, D. A. Day,
1038 and H. Lambers (2004), Developmental physiology of cluster-root carboxylate synthesis and

- 1039 exudation in harsh hakea. Expression of phosphoenolpyruvate carboxylase and the alternative
 1040 oxidase, *Plant Physiol*, 135(1), 549-560, doi:10.1104/pp.103.035659.
- 1041 Sinnott, E. W. (1918), Factors determining character and distribution of food reserve in woody
 1042 plants, *Botanical Gazette*, 66(2), 162-175.
- 1043 Stephens, B. B., P. S. Bakwin, P. P. Tans, R. M. Teclaw, and D. D. Baumann (2007),
 1044 Application of a Differential Fuel-Cell Analyzer for Measuring Atmospheric Oxygen Variations,
 1045 *Journal of Atmospheric and Oceanic Technology*, 24(1), 82-94, doi:10.1175/jtech1959.1.
- 1046 Stringer, J. W., and T. W. Kimmerer (1993), Refixation of xylem sap CO₂ in *Populus deltoides*,
 1047 *Physiologia Plantarum*, 89(2), 243-251.
- 1048 Stumm, W., and J. J. Morgan (1996), *Aquatic chemistry : chemical equilibria and rates in*
 1049 *natural waters*, 3rd ed., xvi, 1022 p. pp., Wiley, New York.
- 1050 Tang, J., and D. D. Baldocchi (2005), Spatial–temporal variation in soil respiration in an oak–
 1051 grass savanna ecosystem in California and its partitioning into autotrophic and heterotrophic
 1052 components, *Biogeochemistry*, 73(1), 183-207, doi:10.1007/s10533-004-5889-6.
- 1053 Teskey, R. O., A. Saveyn, K. Steppe, and M. A. McGuire (2008), Origin, fate and significance of
 1054 CO₂ in tree stems, *New Phytol*, 177(1), 17-32, doi:10.1111/j.1469-8137.2007.02286.x.
- 1055 Tian, W. M., S. G. Yang, M. J. Shi, S. X. Zhang, and J. L. Wu (2015), Mechanical wounding-
 1056 induced laticifer differentiation in rubber tree: An indicative role of dehydration, hydrogen
 1057 peroxide, and jasmonates, *J Plant Physiol*, 182, 95-103, doi:10.1016/j.jplph.2015.04.010.
- 1058 Trumbore, S. (2000), Age of soil organic matter and soil respiration: Radiocarbon constraints on
 1059 belowground C dynamics, *Ecol Appl*, 10(2), 399-411, doi:Doi 10.2307/2641102.
- 1060 Ubierna, N., A. S. Kumar, L. A. Cernusak, R. E. Pangle, P. J. Gag, and J. D. Marshall (2009),
 1061 Storage and transpiration have negligible effects on δ¹³C of stem CO₂ efflux in large conifer
 1062 trees, *Tree Physiology*, 29(12), 1563-1574.
- 1063 Vose, J. M., and M. G. Ryan (2002), Seasonal respiration of foliage, fine roots, and woody
 1064 tissues in relation to growth, tissue N, and photosynthesis, *Global Change Biology*, 8(2), 182-
 1065 193, doi:DOI 10.1046/j.1365-2486.2002.00464.x.
- 1066 Worrall, F., G. D. Clay, C. A. Masiello, and G. Mynheer (2013), Estimating the oxidative ratio
 1067 of the global terrestrial biosphere carbon, *Biogeochemistry*, 115(1-3), 23-32,
 1068 doi:10.1007/s10533-013-9877-6.
- 1069